Template Synthesis of a Facially Coordinated Triphosphine Macrocycle for Biomimetic Hydrogen Production



Dylan G. Boucher

Department of Chemistry

Allegheny College

Meadville, PA 16336

Template Synthesis of a Facially Coordinated Triphosphine Macrocycle for Biomimetic Hydrogen Production

---

Dylan G. Boucher

Senior Comprehensive Project

Allegheny College

4/10/2015

Committee:

Dr. Tim Chapp

Dr. S. Shaun Murphree

Dr. Ann Sheffield

Signature:_____

I hereby recognize and pledge to fulfill my responsibilities as defined in the Honor Code, and to maintain the integrity of myself and the college community as a whole.

Table of Contents

Ackowledgements…… 3

Abstract…… 4

1. Introduction……. 5

1.1 Hydrogenases: Creating Functional Models…… 5

1.2 Template Synthesis: Facially Capped Phopshine Macrocycles…. 11

1.3 Choosing a Template Metal…….. 17

2. Results and Discussion…….. 20

3. Conclusions…… 34

4. Future Work…….. 35

6. Experimental Procedures……. 36

7. References…….. 41

8. Experimental Data…… S0

Acknowledgements

To my mother and father: I can only hope to extend the ceaseless and unconditional support you have shown me to my own children (whenever those things get here…). When I say I love you guys you know I mean it, because you taught me how.

To my brother, John: The funniest person I know and a true a best friend. As you enter this next chapter of your life, I'd like for you to remember one thing: Batman isn't real and your life is lie. Wait, that's two things.

To my friends (which one?): I can always count on you guys to distract me from what I actually need to be doing. Every single one of you has, at one time or another, pulled me away (sometimes forcibly) from work, duties, and responsibilities of all kinds. If it weren't for your imposed degeneracy I would be valedictorian, a published author, and just a generally more effective human being. But you know what? Who needs that junk, I got you guys.

To Jeremy Mason: An excellent mentor, friend, and the reason I actually understand what half of the stuff in a lab does.

To Bob, Brenda, John, and the entirety of the Allegheny College Department of Chemistry: Thank you for making this department what it is and thank you for your efforts to keep it running; it's in great hands.

To Dr. Murphree: I cannot thank you enough for starting me on a journey in pursuit of a passion, a passion that would not exist without your own. You are a constant inspiration for the scientist and educator I hope to be.

To Dr. Chapp: There can be no one more instrumental to this project than you. Your daily guidance, ideas, and enthusiasm have helped me realize why I love what I do, and why I want to do it with the rest of my life. I could not have asked for a better mentor.

And of course,

To my dog, Laurel: Woof (I love you).

Abstract

Preliminary efforts towards a template directed synthesis of a Ni(0) based trisphosphosphine macrocycle for hydrogen activation are underway. 1,3-bis(phenylphosphino) propane was unable to form a stable complex with $Ni(COD)_2$, preferentially forming a mixture of bis-ligated isomers. The mesityl analogue of the ligand, 1,3-bis(mesitylphosphino)propane was synthesized in 20 % yield over two steps and was able to form a stable singly ligated complex, (1,3-bis(mesitylphosphino)propane)Ni(COD). Reaction of this complex with base has resulted in the successful generation of a phosphido intermediate, but formation and isolation of the macrocycle remains to be accomplished.

1. Introduction

In their 2013 International Energy Outlook, the EIA (the United States Energy Information Administration) projected that in the next 30 years, the world's energy consumption will rise by about 56 percent, with almost 80 percent of that energy being provided by fossil fuels.[1] Over the last 20 years, three quarters of all anthropogenic greenhouse gas emissions can be attributed to burning fossil fuels.[2] In an effort to combat the environmental and economic unsustainabilty of fossil fuels, researchers have turned to the possibility of clean burning fuels such as hydrogen. The combustion of dihydrogen, like carbon-based fuels, produces energy but yields only water as its product instead of carbon dioxide. Unfortunately, hydrogen production requires the use of expensive transition metals like palladium or platinum. However, in nature, hydrogen is produced and oxidized by hydrogenase enzymes, which employ first-row transition metals such as nickel and iron in their active sites.[3] Yet, despite the use of first-row transition metals, these enzymes are capable of achieving catalytic rates similar to heavier metal catalysts.[4] Utilization of these first-row transition metals is an attractive option due to their natural abundance and lower toxicity. To this end, work has focused on synthetic analogues that mimic the functionality of these enzymes.[5]

1.1 Hydrogenases: Creating Functional Models

Hydrogenase enzymes catalyze the conversion of dihydrogen into protons and electrons, as well as the reverse: generation of dihydrogen (Scheme 1).

$$H_2(\rightleftharpoons H^+ + H^-) \rightleftharpoons 2H^+ + 2e^-$$

Scheme 1. The reversible, molecular reaction of dihydrogen to protons and electrons. The parantheses specify the heterolytic pathway.[6]

This proceeds through a heterolytic mechanism, either cleavage of dihydrogen into a proton and hydride or the coupling of these species to generate molecular dihydrogen. In the enzyme, heterolytic cleavage is facilitated by the increased acidity of dihydrogen due to the transition metal center and a nearby base to accept or deliver the protons; this heterolytic mechanism has been supported by isotope exchange experiments.[7] Utilization of the heteorolytic pathway (two electron reduction) as opposed to the homolytic pathway (single electron reduction proceeding through a radical intermediate) minimizes the energy barrier of the reaction.[8]

In nature, these hydrogenases come in three varieties: [FeFe], [NiFe], and [Fe] (Chart 1),

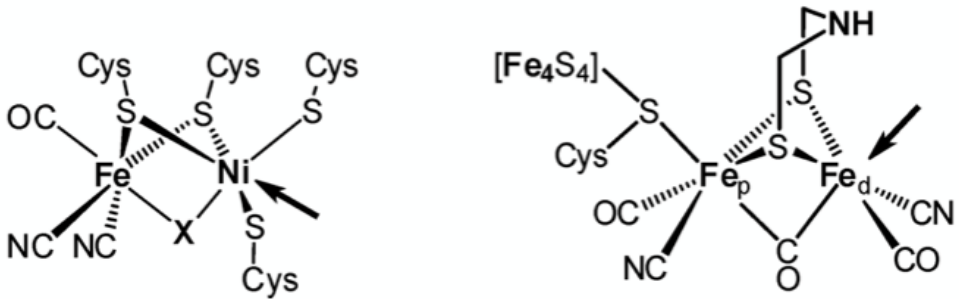


Chart 1. Active sites of [FeNi][10] and [FeFe][11] hydrogenase enzymes. Arrows denote open coordination sites available for binding dihydrogen.

---

though [Fe] hydrogenase can only activate H_2 for the reduction of a specific substrate[9] and thus does not represent a suitable model for H_2 production. [NiFe] has shown greater activity for oxidation of dihydrogen, while [FeFe] hydrogenases typically favor the generation of dihydrogen.[6] Thus, [FeFe]-hydrogenase is the most ideal of the hydrogenase family for biomimetic modeling of hydrogen production. [FeFe]-hydrogenase's high activity for hydrogen production is due to a number of notable structural features. The active site possesses a pendant amine in the secondary coordination sphere which acts as a base to facilitate proton delivery to

the metal center. The metal center is ligated by unusually strong-field groups, such as carbon monoxide and cyanide, which possess low-lying pi-orbitals that accept electron density from the metal center. The result of this strong ligation is increased lewis acidity of the metal. These ligands also create a unique electronic environment due to their facial coordination in comparison with the weaker-field sulfur ligands. Since the facially coordinated, strong-field ligands sit opposite of the open coordination site on the metal, this site sees increased lewis acidity, priming it for hydrogen activation. In addition, the active site is covalently bound to an iron-sulfur cluster (Fe_4S_4), which acts as part of an electron relay to transport electrons from the surface of the enzyme to the active site (Chart 2).

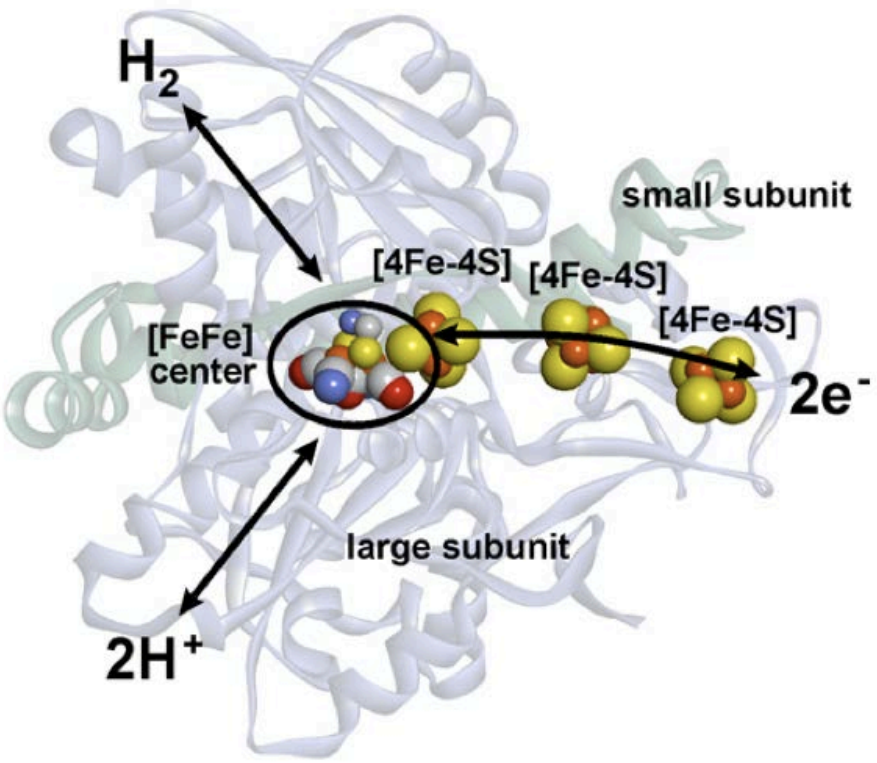
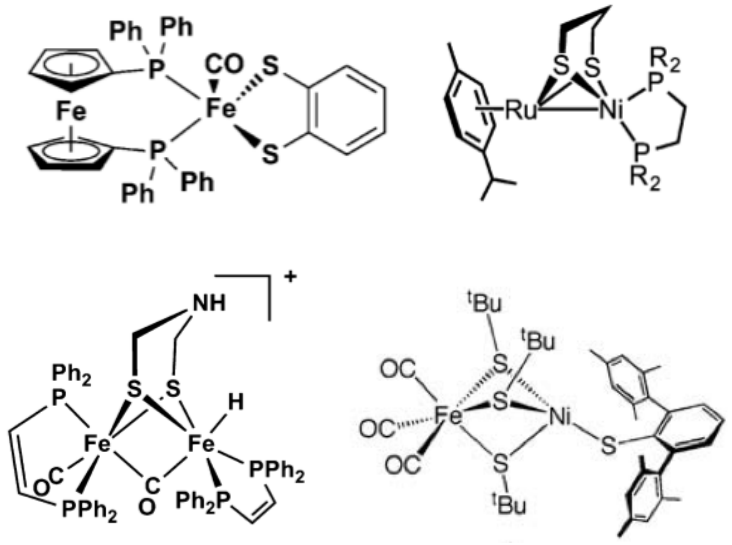


Chart 2. Full [FeFe] hydrogenase enzyme with protein structure highlighting the active site, electron relay, and proton and dihydrogen pathways.[6]

Biomimetic modeling of these enzymes has evolved as a way to translate their catalytic activity and specificity into a small-molecule format without the need for the protein substructure. Utilizing ligands and metal salts, coordination complexes that incorporate salient structural and chemical motifs of the enzymes' active sites have been synthesized (Chart 3) and shown to exhibit similar functionality.[12-14]



a **b**

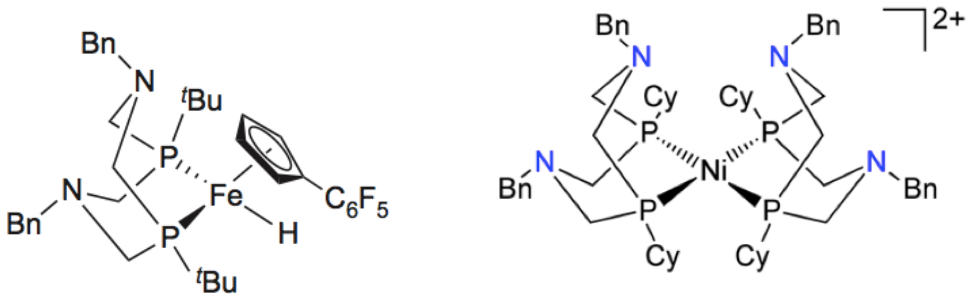
Chart 3. Examples of previously reported synthetic mimics of **a)** [FeFe][12,15] and **b)** [NiFe][13,14] hydrogenase active sites.

In many cases, faithful structuring of the active site leads to dramatic increases in catalytic activity, chiefly the incorporation of the pendant amine structure of the [FeFe]-hydrogenase's second coordination sphere. Rauchfuss *et al.* showed that incorporation of this feature into their synthetic model dramatically increased the catalytic rate constant over those complexes not featuring the amine.[15] This pendant amine acts as a proton relay during catalysis, removing or delivering protons to the metal center.[16] Its function as a proton relay is essential to the effective

operation of the [FeFe]-hydrogenase in nature and is clearly an important structural component to incorporate into small molecule models.

Because of their molecular scale and participation in the hydrogen half reaction, these biomimetic catalysts are classified as molecular electrocatalysts. As such, evaluation of these catalysts is performed in a half-cell reaction scheme, with the electrons being supplied by an electrode and protons from an acid. Catalytic rate constants, turnover frequencies, and oxidative states can be determined by electroanalytical methods such as cyclic voltametery.[17]

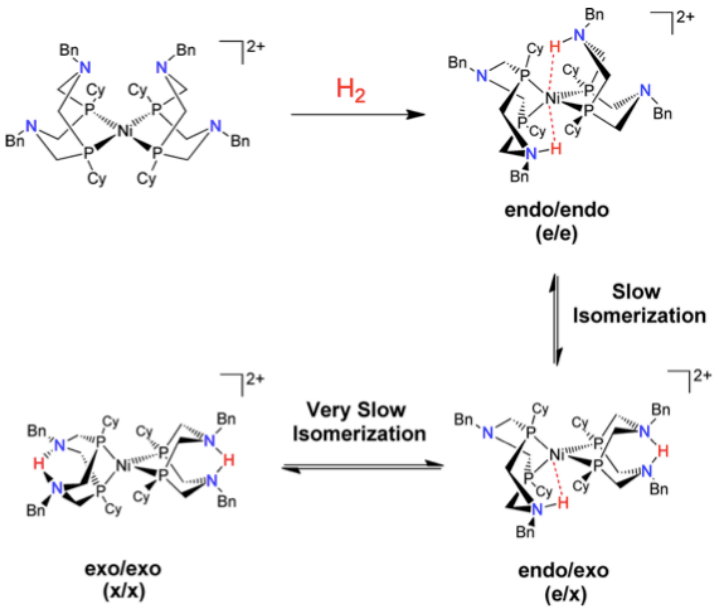
The pendant amine structural motif has become a major feature in some of the fastest molecular electrocatalysts for hydrogen production, including a class of catalyst explored extensively by DuBois *et al*. DuBois' catalysts employ diazodiphosphine macrocyclic ligands with first row transition metals to generate complexes (Chart 4) capable of extremely high turnover frequencies.[18] These catalysts pair the simplicity of a mononuclear metal complex of one or two bidentate ligands with the catalytic power of the hydrogenase enzymes. Though these catalysts eschew faithful replication of the hydrogenase active site for structural simplicity, their biologically inspired design has led to some of the most promising turnover frequencies for molecular catalytic hydrogen production.



a **b**

Chart 4. Examples of DuBois' catalyst structure with **a)** Fe metal center[19] and **b)** Ni center.[20]

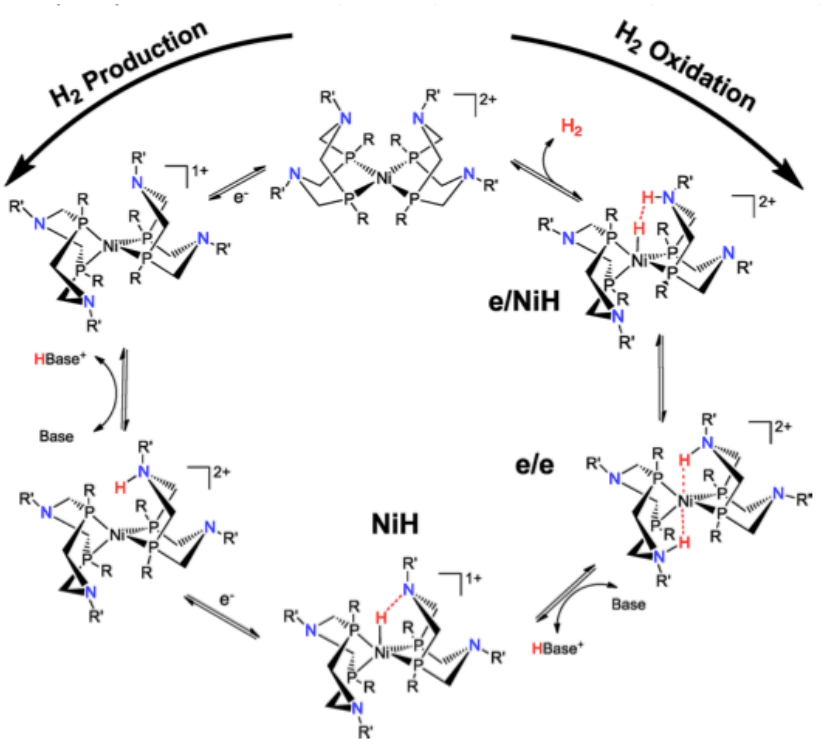
DuBois' complex activates molecular hydrogen (hydrogen oxidation, the reverse of hydrogen production) which ultimately equilibrates over the course of several days into three isomers[20] (Scheme 2).



Scheme 2. Possible isomers of the DuBois catalyst. Optimal catalysis requires the *endo* position which is not the kinetically preferred isomer.

Of these isomers, the endo/endo configuration is catalytically active, as it situates the pendant amine close to the metal center for optimal proton delivery. However, hydrogen production requires the reverse reaction to occur: protonation of the pendant amines (Scheme 3). Reacting the complex with two equivalents of acid resulted predominantly in the formation of the exo/exo product thereby showing that the catalytically inactive isomer is the kinetically favored product of protonation. Since the catalytic cycle for hydrogen production entails an initial protonation of the complex, isomerization from the kinetically favored exo/exo isomer to the catalytically active endo/endo isomer is likely a major rate-limiting factor. Overcoming this obstacle means

optimizing the sterics and coordination of the catalyst such that the *endo* isomer is kinetically preferred.

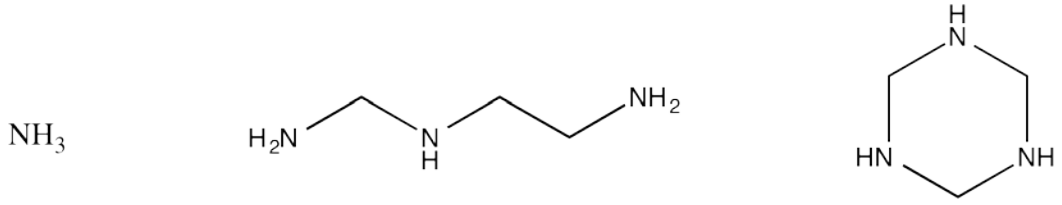


Scheme 3. Catalytic cycle of the DuBois' complex for both hydrogen production and oxidation.

1.2 Template Synthesis: Facially Capped Phosphine Macrocycles

If the catalyst is locked into the *endo* position by tight control of molecular geometry, then rate of catalysis will increase. Thus explicit control of coordination geometry around the metal is crucial to the development of an optimal catalyst. Molecular geometry dictates reactivity of transition metal catalysts, as spatial positioning of open coordination sites for reactants is crucial to the specificity of a catalyst. In this case, molecular geometry dictates the pendant amine's access to the metal center. The molecular geometry of metal complexes is largely governed by the metal and its oxidation state; in other words, the d-electron count of the metal. However, substantial influence over the geometry of a complex can be exerted by ligand type.

High field and low field donors can affect orbital splitting and thus electron configuration. Likewise, the sterics of a ligand can substantially impact its coordination number, for example a large, sterically hindered ligand may prevent the coordination of other ligands, despite the fact it may be energetically favorable to form a complex with a higher coordination number. Multi-dentate ligands can also impact the coordination geometry of a metal complex. By connecting the donor atoms covalently, specific spatial configurations are enforced. The size and rigidity of the covalent backbone determines the relative position of the donor atoms, also called the bite angle, which plays an important part in determining the overall molecular geometry. One prominent class of multi-dentate ligands are macrocyclic ligands. Coordination chemists define macrocycles as cyclic compounds with three or more donor atoms. Macrocyclic ligands offer a number of advantages over mono-dentate, bidentate, and non-cyclic tridentate ligands. For example, just as the chelate effect dictates that a bidentate complex is more stable than its monodentate anaglogue, the macrocyclic effect offers further stability to a macrocyclic complex over both the single and open chain counterparts (Chart 5).



a **b** **c**

Chart 5. Example of monodentate (**a**), tridentate open chain (**b**), and tridentate macrocyclic (**c**) ligands.

In addition, a macrocyclic ligand imposes greater restrictions on the geometry of a coordination complex in comparison to a linear (non-cyclic) ligand. Whereas a linear ligand may form either

the the *fac* (facial) or *mer* (meridional) isomers (Chart 6), a macrocyclic ligand will most likely assume a facial configuration, keeping the donor atoms closest to alleviate strain on the cycle that connects them.

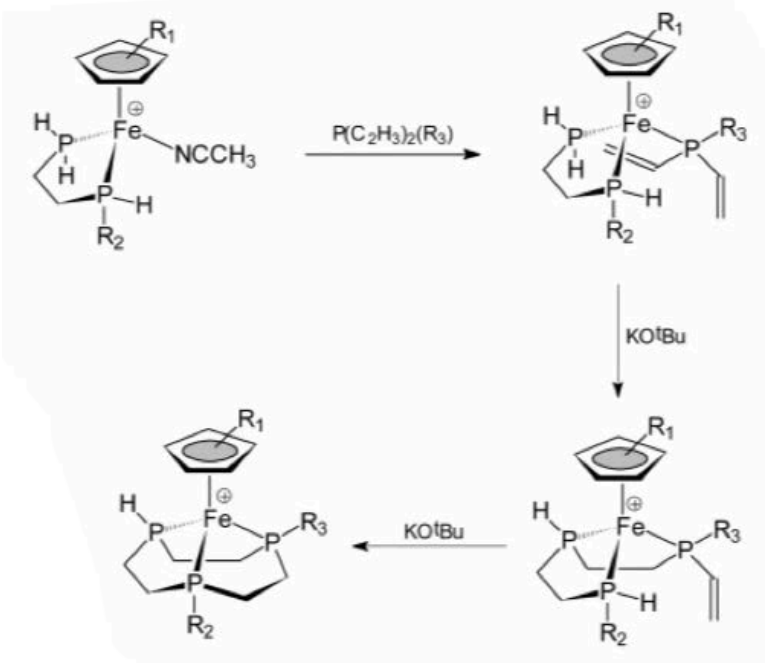


fac ***mer***

Chart 6. General depiction of facially (*fac*) and meridional (*mer*) octahedral isomers. L is a general ligand and blue or red coloration differentiates the ligand groups (for example: the same ligand or donor atoms from a single molecule).

One way coordination can be controlled synthetically is through a template synthesis. Template syntheses utilize coordination of multiple ligands around a metal center, which can then be reacted to form a macrocycle between the ligands. Known as the template effect, the pre-organization of reactants around the metal center makes the cyclization product kinetically favorable and diminishes byproducts, which, without the template, would be the dominant product. In addition, this method of ligand design imposes structural restrictions on the geometry of the metal center through the bite angles of the beginning ligands[21] and is capable of producing facially capped tri-dentate macrocycles[22-24] (Scheme 4). The result of this templated

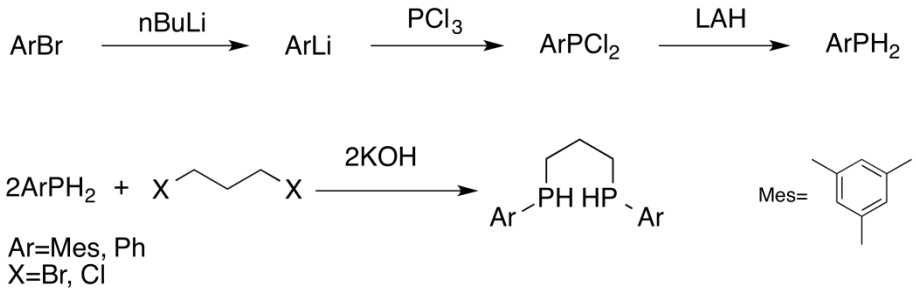
route is a kinetically favored, energetically stable complex that ties the phosphine atoms back leaving an open site for hydrogen activation.



Scheme 4. Example of a templated formation of a macrocycle utilizing Fe(II) as a template.[22] Activation of the vinyl groups is a base-catalyzed Michael-type addition to the secondary bisphosphine.

One drawback to this method of ligand design however, is the difficulty of releasing the metal template from the macrocycle.[25] However, template syntheses are often conducted using abundant first row transition metals such as iron[22-23] and nickel.[26] Thus, a templated synthetic route is ideal for developing a first-row transition metal based catalyst as there will be no need to release the metal after formation of the macrocycle. It becomes important then to choose the proper metal template that will provide proper catalytic function, oxidative state, and molecular geometry after complexation and formation of the macrocycle.

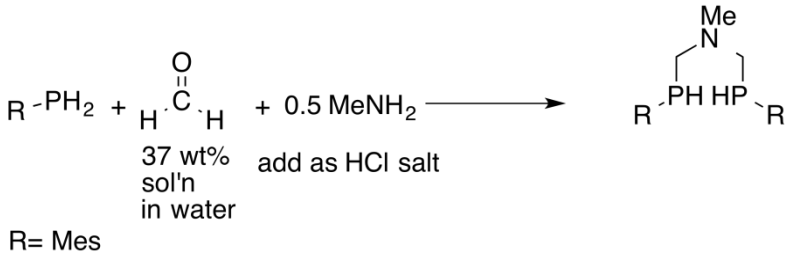
Phosphine-based ligands are ideal for transition metal catalysts due to their steric and electronic tunability thereby allowing control over the catalyst's reactivity.[27] Phosphine donors are also ideal from a biomimetic perspective. The hydrogenase enzyme's active site is comprised of many strong-field ligands such as cyanide and carbon monoxide. Phosphine donors are also strong-field ligands, making a phosphine macrocycle a better choice than other common macrocyclic donors, such as amines which are a mid-field ligands. Thus a phosphine-based macrocycle would allow for both steric and coordinative control in the design of a transition metal based catalyst that accurately reproduces the hydrogenase active site in terms of ligand field strength. Template syntheses of polydentate phosphine macrocycles utilizing first row transition metals are relatively common.[22-26] These syntheses typically employ a secondary bisphosphine ligand and a tertiary aryl divinyl phosphine templated to a transition metal center (Scheme 4); the vinyl groups can then be activated via base-catalyzed Michael-type addition[22] or radical initiated addition[23] to the secondary phosphines, thereby generating the phosphine macrocycle. Secondary bisphosphine ligands (secondary phosphines bridged by an alkyl chain) are easily accessible through substitution reactions between primary aryl phosphines and dihalogenated alkanes[28] (Scheme 5).



Scheme 5. General Synthetic route to primary aryl phosphines and secondary bisphosphine ligands.

Likewise, polyvinyl phosphines are accessible through reaction of the appropriate equivalents of vinyl magnesium chloride and tri- or diphenyl phosphite .[29]

The pendant amine structural motif can also be incorporated into a phosphine macrocycle through the condensation of a secondary bisphosphine ligand with formaldehyde and a primary amine in a Mannich-style reaction.[28] However, this is a non-templative synthesis, and subject to the same suboptimal coordination of the DuBois' catalyst (Scheme 2). Templative synthesis of a pendant amine containing phosphine macrocycle has yet to be explored, but there is precedent for incorporating pendant amine functionality into the alkyl bridge of a secondary bisphosphine ligand through another Mannich style reaction: condensation of the primary phosphine with formaldehyde forms a secondary hydroxyalkylphosphine intermediate which reacts with 1 equivalent of a primary amine[30] to form the secondary bisphosphine with the pendant amine as a heteroatom in the bridge between the two phosphine donors (Scheme 6).



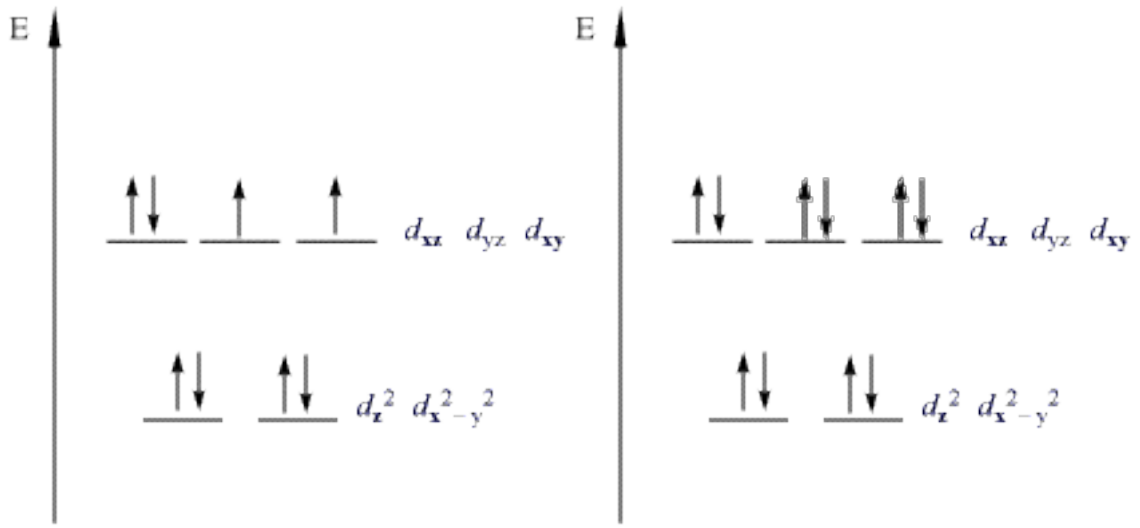
Scheme 6. Proposed synthesis of a pendant amine containing secondary bisphosphophosphine ligand.

This would have to be done on a substantially bulky primary phospine (such as mesitylphosphine) to suppress phosphine condensation with two equivalents of formaldehyde.

1.3 Choosing a Template Metal

As discussed earlier, template syntheses can be conducted on a wide range of first-row transition metals in various oxidation states. Releasing the template metal after formation of the macrocycle is often difficult, therefore it is imperative to choose a metal center that affords the most useful catalytic activity, oxidation state, and molecular geometry. The desired geometry is tetrahedral both to more accurately mimic the geometry of the hydrogenase active site and, by extension, improve the catalytic efficacy by leaving the open coordination site near the pendant amine. Therefore iron and nickel are both suitable template metals as both are capable of tetrahedral geometries in four coordinate systems. Iron would be the logical choice as [FeFe]-hydrogenase is the most active of the hydrogenases for catalytic hydrogen production. Yet, nickel is in the same group as both Pd and Pt, the preeminante catalysts for industrial hydrogen production. Indeed, the nickel variant of DuBois' catalyst is capable of higher turnover frequencies than the iron analogue, which has a higher activity for hydrogen oxidation.

For catalytic efficacy, nickel is the more suitable option. There is precedent for template synthesis of triphoshine macrocycles using nickel(II),[26] however in the tetrahedral geometry desired, a nickel(II) complex would be paramagnetic (Chart 7)



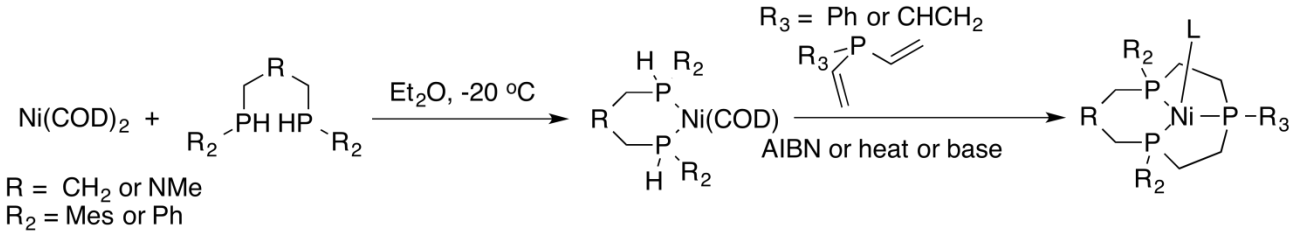
Ni(II) **Ni(0)**

d8 **d10**

Chart 7. D-orbital splitting of tetrahedral Ni(II) which is paramagnetic and Ni(0) which is diamagnetic.

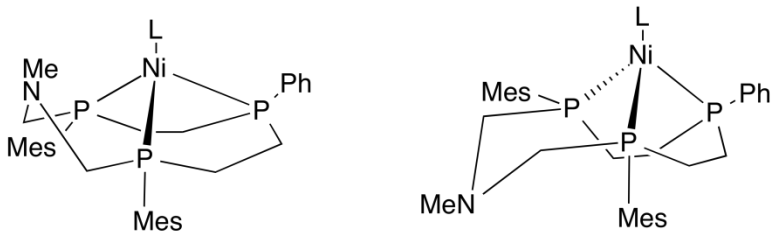
---

making characterization challenging (requiring the use of EPR spectroscopy). Nickel(0) then provides a much more attractive template as it would be predicted to be diamagnetic in a tetrahedral geometry and can be characterized by NMR. Bisphosphine Ni(0) complexes are relatively common.[31,32] Though nickel(II) is more common for template syntheses, Hafner *et al*'s synthesis of a three coordinate nickel(0) complex using a bisphosphine ligand and butadiene[32] suggests that this route could be exploited for the template synthesis of a trisphosphine macrocycle through the intermediary nickel(0) bisphosphine divinylphosphine complex (Scheme 7).



Scheme 7. Proposed templative synthesis of the phosphine macrocycle utilizing Ni(0) and proceeding through a three coordinate intermediate. The coordination site for hydrogen activation is the general ligand site designated *L*.

A nickel(0) facially-capped triphosphine macrocycle leaves an open coordination site for hydrogen activation, and nickel(0) has been shown to activate dihydrogen, even without the pendant amine structure, though hydrogen activation is more thermodynamically favorable if the pendant amine is included.[31] In addition, the phosphine donors of the macrocycle are open to steric tunability allowing modification of the macrocycle to ensure that the pendant amine structure favors the *endo* position (Chart 8).



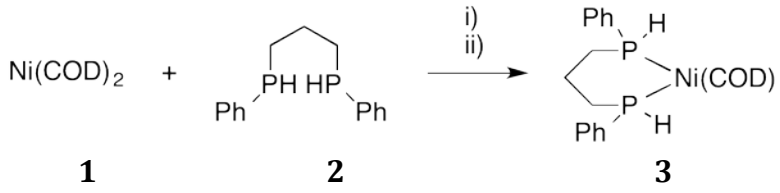
endo ***exo***

Chart 8. Proposed geometry of the Ni(0) facially-capped triphosphine macrocycle complex with the pendant amine in the *endo* position and the competing *exo* position. The combined steric bulk of the mesityl groups and restrictive geometry of the macrocycle are expected to make the *endo* position more favorable.

Thus, combining the restrictions on geometry imposed by a macrocycle such as this along with bulky substituents on the phosphine donors will rigorously enforce the *endo* position and increase the rate of catalysis.

2. Results and Discussion

Initial attempts at synthesizing a nickel(0) secondary bisphosphine complex (**3)** utilized bis(cylcooctadiene)nickel(0) (**1)** as a source of nickel(0) and 1,3-bis(phenylphosphino)propane (**2)** as the secondary bisphosphine ligand (Scheme 8).



1 **2** **3**

Scheme 8. Initial attempts at the synthesis of a secondary bisphosphine Ni(0) complex. i) THF, room temperature. ii) THF, -20^{o}C. Neither conditions afforded the nly the singly ligated complex.

Metallation was attempted at both room temperature and at -20^{o}C. At room temperature, metallation resulted in a dark brown solution (atypical of the usual yellow or orange of Ni(0) complexes) . The resulting ^{31}PNMR spectrum (Chart 10) showed wide range of signals However, the majority of phosphorus signals were a group of multiplets ranging from around -7 ppm to -10 ppm attributed to the mix of isomers possible from double ligation (Chart 9).

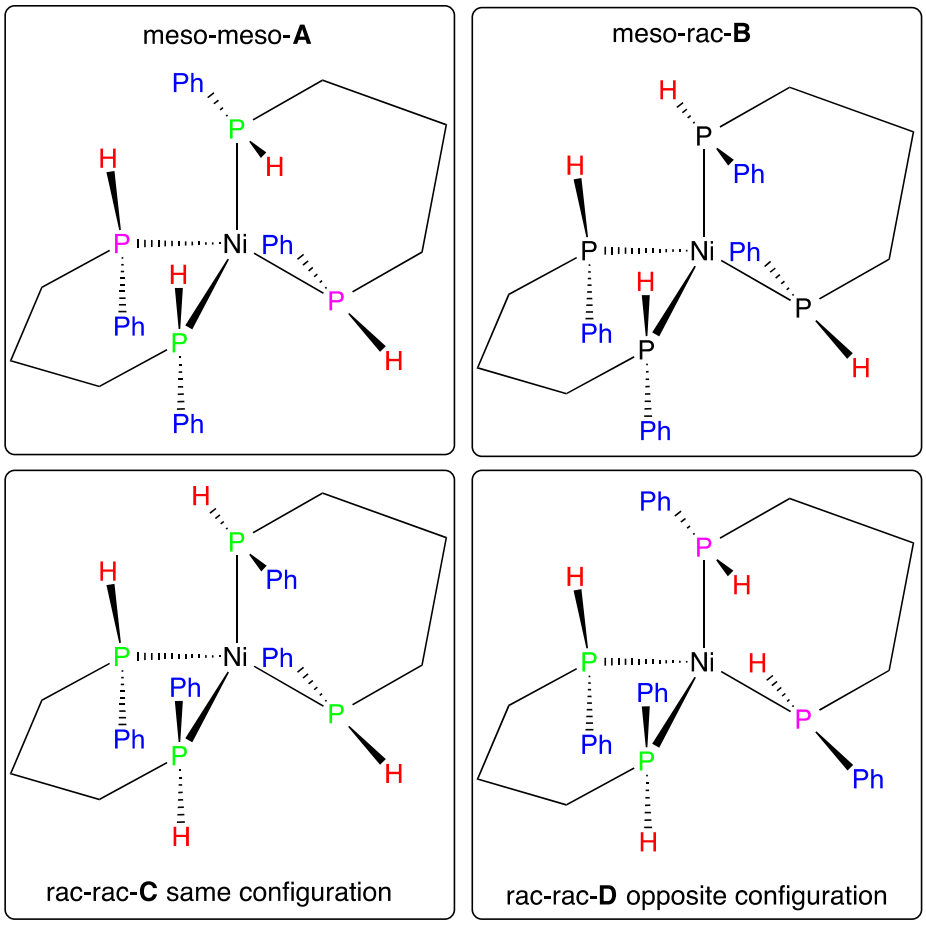


Chart 9. Possible isomers formed from bis-ligation of the metal.

Isomer A is assigned a C_2 point group allowing for two kinds of P-P coupling suggesting a resulting doublet of doublets. However the intraligand coupling can be very small, and can simplify to a doublet. Thus the isomer is assigned a doublet (of which both peaks are broad which could be the result of intraligand coupling) centered on 3.52 ppm. For isomer B (point group assigned C_1) all of the donor phosphines are in chemically inequivalent environments suggesting a resulting complicated multiplet, thus this isomer is assigned the broad set of multiplets ranging from -7.82 to -9.25 ppm. Isomer C is assigned a D_2 point group and is chiral, thus the phosphine donors are all in chemically and magnetically equivalent environments (thus

no P-P coupling) allowing it to be assigned to the singlet at 2.02 ppm. Finally, isomer D can be assigned the S_4 point group. As such, the phosphine donors on their respective ligands are equivalent, suggesting a resulting triplet, whereby one phosphine is split by the other two. Therefore, isomer D is assigned the triplet at -7.06 ppm. These assignments leave two prominent signals at -7.81 ppm and -10.10 which are assigned to the *rac* **(a)** and *meso* **(b)** isomers respectively of the desired product (Chart 11).

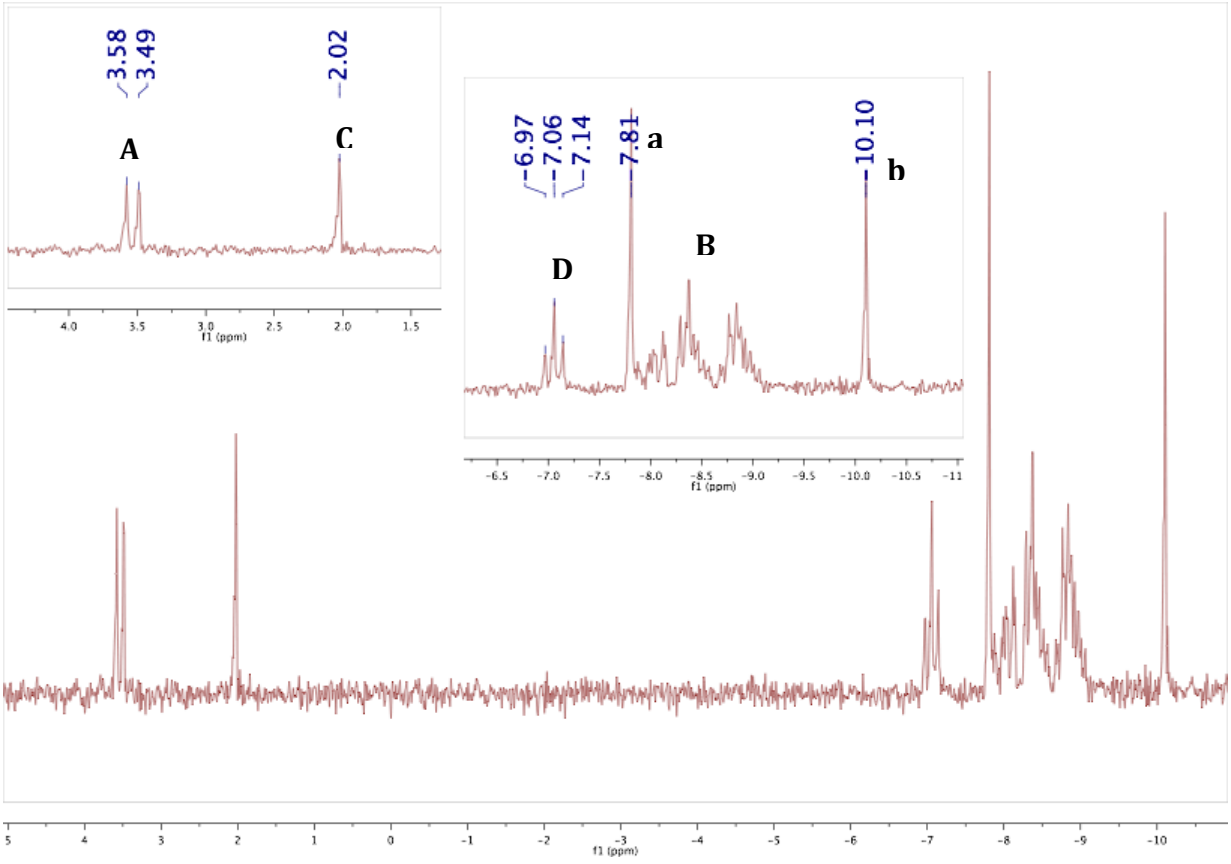
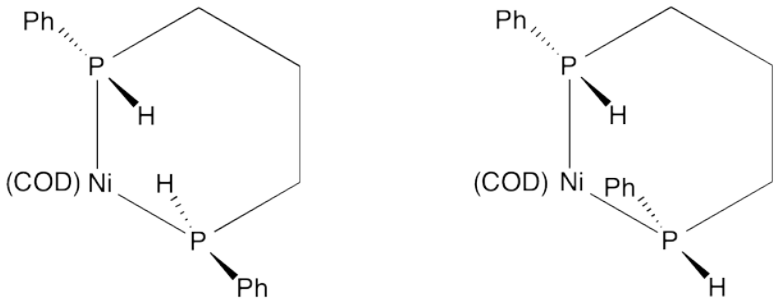


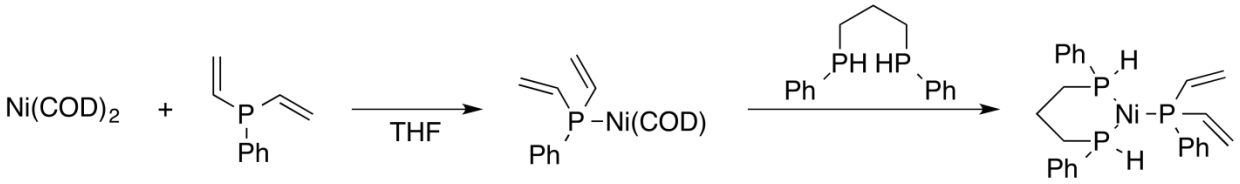
Chart 10. ^{13}PNMR spectrum with proton decoupling summarizing isomer assignments. Insets are magnifications of regions of interest.



***rac* (a)** ***meso* (b)**

Chart 11. Two possible isomers of the singly ligated complex, **3**

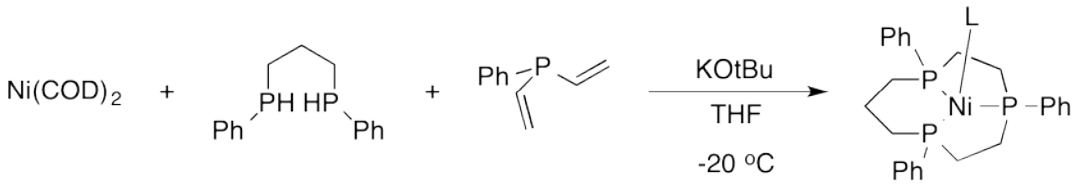
Metallation performed at -20°C formed a yellow solution, however when warmed to room temperature, the same results were obtained.



1 **4** **5** **6**

Scheme 9. Attempted metallation to block multi-ligation of the secondary bisphosphine ligand.

An attempt to lock up one coordination site and prevent multi-ligation was carried out by reacting nickel(0) with divinylphenylphosphine (**4**) followed by addition of **2** (Scheme 9). Upon addition of the **4** to **1** a color change from yellow to orange was observed, accompanied by a prominent phosphorus peak at 16.9 ppm indicating successful coordination. However upon addition of **2**, the same dark brown solution with accompanying spectra was observed. In addition, precipitate is observed presumed to be Ni(0). The successful coordination **4** and the presumed stability of the singly ligated complex at low temperature prompted exploration of a single pot synthesis of the macrocycle (Scheme 10)

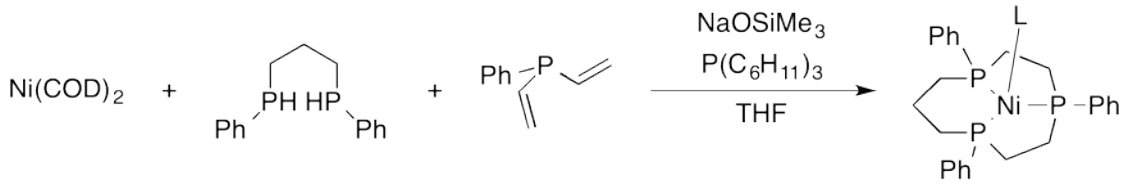


1 **2** **4** **7**

Scheme 10. Attempted one pot synthesis of the macrocycle at low temperature activated by the base, KOtBu.

After stirring for 24 hours, ^{31}PNMR showed only wide, scattered multiplets with low signal to noise ratio suggesting the possibility of polymerization of **4**.

Further steps were taken to prevent unstable intermediates to keep Ni(0) in solution with the addition of one equivalent of tricyclohexylphosphine (**8**) (Scheme 11).



1 **2** **4** **7**

Scheme 11. Attempted one pot synthesis with $NaOSiMe_3$ as the base and tricyclohexylphosphine to keep Ni(0) in solution.

The resulting spectra without base (Chart 12) showed no evidence of bis-ligated isomers **A** and **B**, and left the presence of **D** ambiguous, suggesting that tricyclohexylphosphine is competitive in the formation of these isomers. Most interestingly, the new spectra showed a decrease in only one of the peaks attributed to singly ligated diastereomers, suggesting that **4** selectively

coordinates to only one isomer, most likely the *meso* isomer (the peak at 10.10 ppm), due to steric hindrance of the phenyl groups in the *rac* isomer.

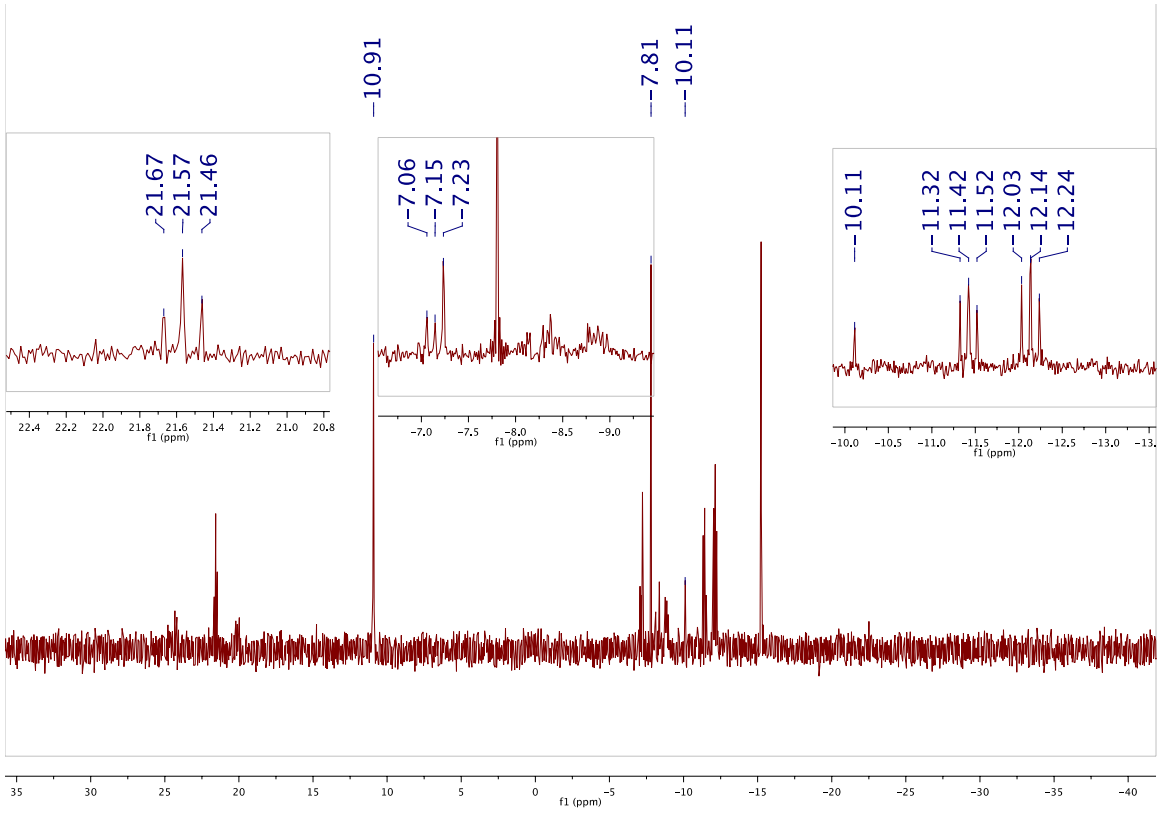


Chart 12. Resulting ^{13}PNMR spectrum from the attempted one pot synthesis of the macrocycle utilizing tricyclohexylphosphine to increase solubility of intermediates.

There was also the appearance of what may be two triplets or overlapping doublet of doublets at 21.57, -11.42 ppm, -12.14 ppm. Selective coordination of **4** to the *meso* isomer of the singly ligated complex would be expected to yield similar signals.

Species	**Chemical Shift (ppm)**
$P(C_6H_{11})_3$	10.91 (s)
$P(CHCH_2)_2Ph$ (**4**) (unbound)	-15.23 (s)
Rac isomer (**3a**)	-7.81 (s)
Meso isomer (**3b**)	-10.10 (s)
Bis-ligated Isomer D	-7.06 (t)
Bis-ligated Isomer B	-7.82 to -9.25 (m)
Three coordinate intermediate (**6**)	21.57 (t), -11.42 (t), and -12.14 (t)

Table 1. Summary of ^{31}PNMR assignments from chart 12.

The addition of base to this mixture (after 48 hours of stirring) (Chart 13) resulted in the total elimination of the bis-ligated isomers. The signals still present include $P(C_6H_{11})_3$ at 10.91 ppm and the *rac* singly ligated isomer at -7.77 ppm (-7.81 in the previous spectrum). The broadening of the peak at -15.23 ppm indicates polymerization of **4**. Only traces of the triplets (or overlapping double doublets) at 21.57 ppm, -11.42 ppm, and 12.14 ppm remain. However a new peak appears at -7.19 ppm which is roughly consistent with the chemical shift of Helm's free macrocycle [33]. This signal could potentially correspond to the free macrocycle whereby the macrocycle forms and does not stay bound to Ni(0). If it is the macrocycle, it is unclear why it does not stay bound to Ni(0), suggesting perhaps that the atomic radius of Ni(0) may be too large to result in successful coordination of the macrocycle (Table 2). Isolation of this signal was attempted but unsuccessful and ultimately abandoned to pursue the less complex reaction mixtures metallation of the mesityl bis-secondary phosphine ligand affords.

Metal	Ni(0)	Ni(II)	Fe(II)
r (Å)	1.35	0.83	0.75

Table 2. Empirical values for the atomic radii of metals used for template syntheses.[34] The size of Ni(0) may be inhibiting formation of the macrocycle

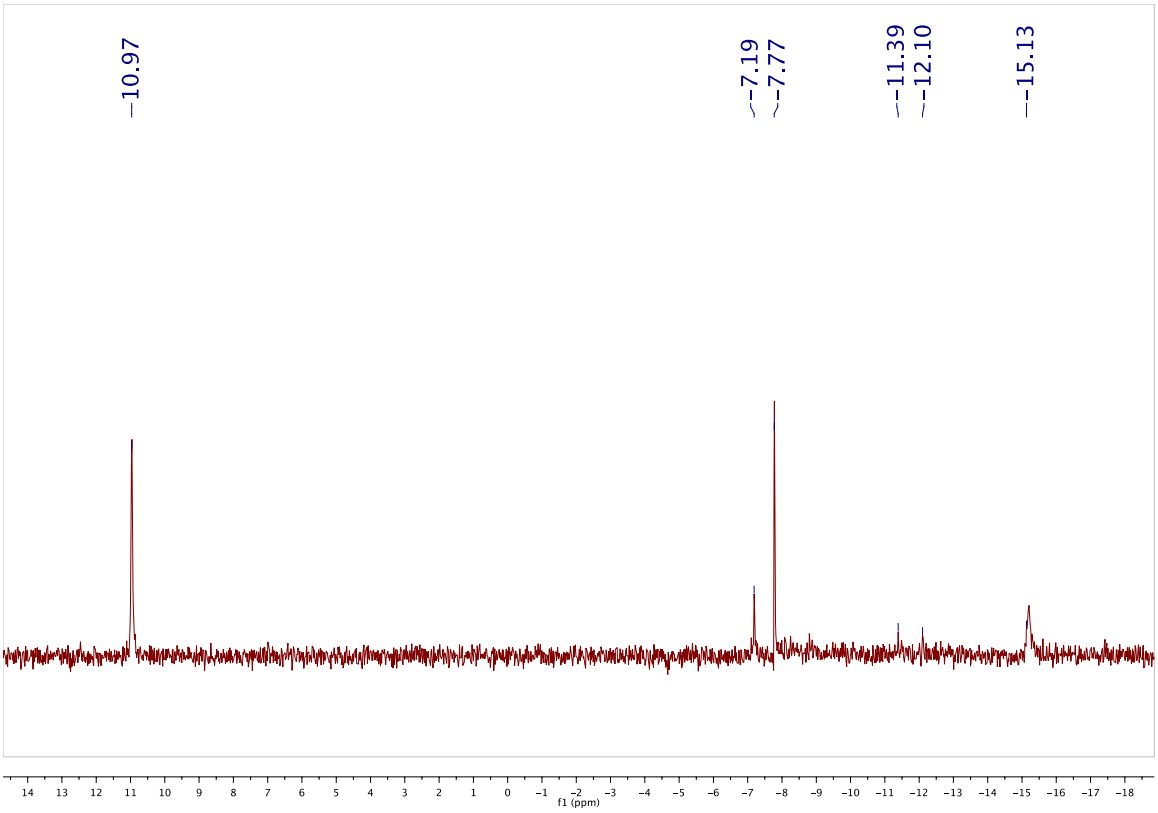
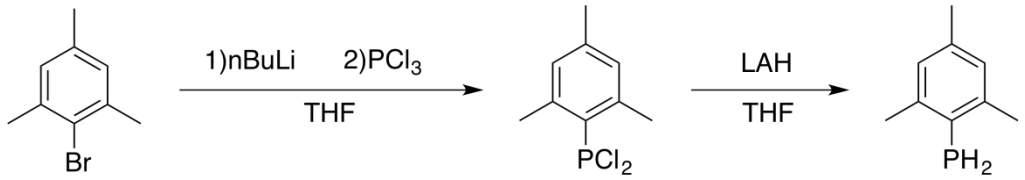


Chart 13. Spectrum of the attempted one pot synthesis of the macrocycle after the addition of base and stirring for 48 hours.

On that front, these experiments indicated that the secondary 1,3-bis(phenylphosphino)propane ligand is not a strong enough donor to produce a stable, singly ligated complex (whereas the tertiary analogue is a known compound). To overcome this,

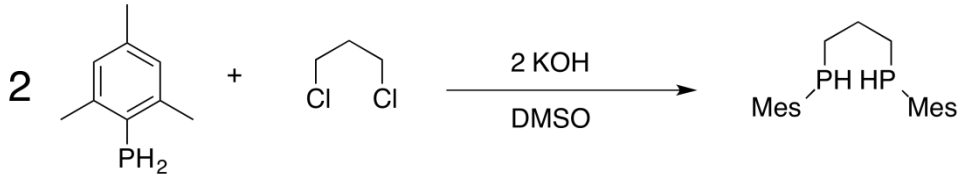
synthetic efforts were directed towards the mesityl analogue of the ligand, 1,3-bis(mesitylphosphino)propane (**13**) under the rationale that the electron donating methyl groups of the mesityl substituents will increase the electron density of the phosphorus donors and increase stability of the coordination to nickel(0) and prevent the formation of bis-ligated isomers.



8 **9** **10**

Scheme 12. Synthesis of mesitylphosphine from 2-bromomesitylene. Yield over two steps was 67.7%

The primary mesitylphosphine (**10**) was synthesized consistently in 65-70% yield over two steps (Scheme 12). This reaction was carried out in a single pot without purifying the mesitylphosphonous dichloride (**9**) intermediate. Both steps were monitored easily by NMR spectrscopy.

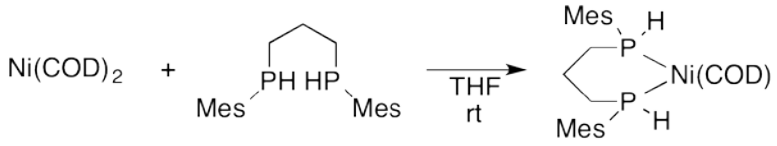


10 **11** **12**

Scheme 13. Synthesis of secondary 1,3-bis(mesitylphosphino)propane ligand.

---

10 was taken forward to synthesize the secondary bisphosphine ligand (**12)** (scheme 13). Initially, 1,3-dibromopropane was used as the source of the alkyl link between the phosphine atoms. However, ^{31}PNMR monitoring of this reaction showed a dramatic downfield shift, further than anticipated, indicating overalkylation of the phosphine. To combat this, 1,3-dichloropropane (**11**) was used in place of the dibromo analogue to slow down the rate of substitution, which resulted in the product **12**. The product was purified by kugelrhor distillation to give the product in 29% yield. The low yield is mostly due to product loss in distillation.

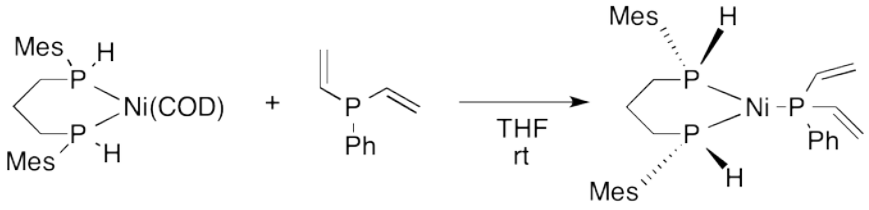


1 **12** **13**

Scheme 14. Synthesis of the mesityl analogue of the bis-secondary phosphine complex. ^{31}PNMR showed formation of only the singly ligated complex. Stereochemistry is not specified here, as both *rac* and *meso* isomers are observed.

---

12 was taken forward and metallated with **1** at room temperature. The hypothesis proved correct as the ^{31}PNMR showed a clean spectrum with only the expected diastereomeric singlet peaks at -21.40 ppm and -26.20 ppm for the *rac* and *meso* isomers of the singly ligated complex.



13 **4** **14**

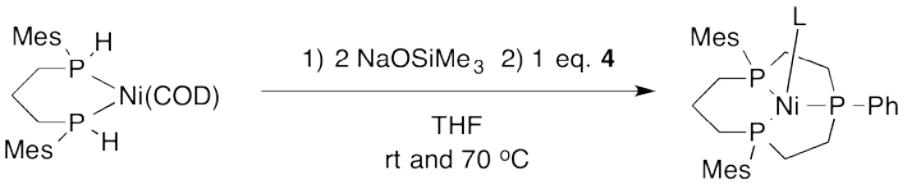
Scheme 15. Coordination of **4** to the singly ligated bis-secondary complex. Due to the steric bulk of the *rac* isomer, only the *meso* isomer could bind **4.**

Peak (ppm)	Integral before addition of 4	Integral after 4
6.58	Not Present	0.26
-21.40	1.0	1.0
-26.20	0.97	0.75
-32.05	Not Present	0.20
-38.08 (d), -44.38 (d)	Not Present	0.40, 0.17
-39.966 (d)	Not Present	0.44

Table 3. Summary of the changes in ^{31}PNMR spectrum with the addition of **4** to a solution of **13**. The coupling constant of the doublets centered at -38.08 ppm and -44.38 ppm is the same, thus they are purported to correspond phosphine atoms on the same compound. All integrals normalized to 1.0.

Addition of one equivalent of **4** with the singly ligated complex led to a decrease in only one of the diastereomeric peaks, further supporting the previous observation with the phenyl analogue that the sterics of the *rac* isomer render it incapable of binding **4**. In addition, two doublets with identical coupling constants appear at -38.08 ppm and -44.38 ppm with integrals that are roughly 2:1, these peaks are consistent with the signals that would be expected for **14** since the secondary phosphines of the active *meso* isomer are equivalent. However, the other doublet (at -39.66 which does not share a coupling constant with the previous two doublets) and the singlets at 6.58 ppm and -32.05 indicate a complex mixture of compounds. After stirring for 24 hours, the ^{31}PNMR spectrum showed only the diastereomeric peaks of **13** (with an integration of 1 to 0.62) and a broad swath around 30 ppm suggesting polymerization of **4** and any species to which it

was bound; polymerization is supported by the fact that nickel-based systems are often used to catalyze polymerization of alkenes.[35,36]



14 **15**

Scheme 16. Attempted synthesis of the macrocycle through a bis-phosphido intermediate. Reaction was performed both at room temperature and 70 ^{o}C.

To avoid polymerization, the singly ligated complex was reacted with two equivalents of base to generate the bis-phosphido intermediate (Scheme 16), however the complex proved to be very stable and after an hour of stirring and an extra equivalent of base, the NMR spectrum still showed the protonated, diastereomeric peaks. Addition of **4** to the reaction mixture at room temperature after 48 hours of stirring revealed the appearance of several new peaks (Chart 14), including what appears to be two triplets or overlapping double doublets at -17.89 ppm and -40.59 ppm (the peak at 94.20 ppm is an impurity present in the starting materials) with the same coupling (30 Hz) indicating that these signals are connected. The peak at -40.59 is consistent with observed chemical shifts of terminal phosphido ligands.[37] However, the connected peak at -17.89 indicates that this likely not a bis-phosphido intermediate. Two possible structures for this single phosphido intermediate (Scheme 15) are **16** and **17**. **16** would be the result of deprotonation of one the secondary phosphine donors. Considering the stability of the complex in the presence of base however, a more likely case is **17** which would result from oxidative addition across the phosphorus-Ni bond which is a common motif in catalytic

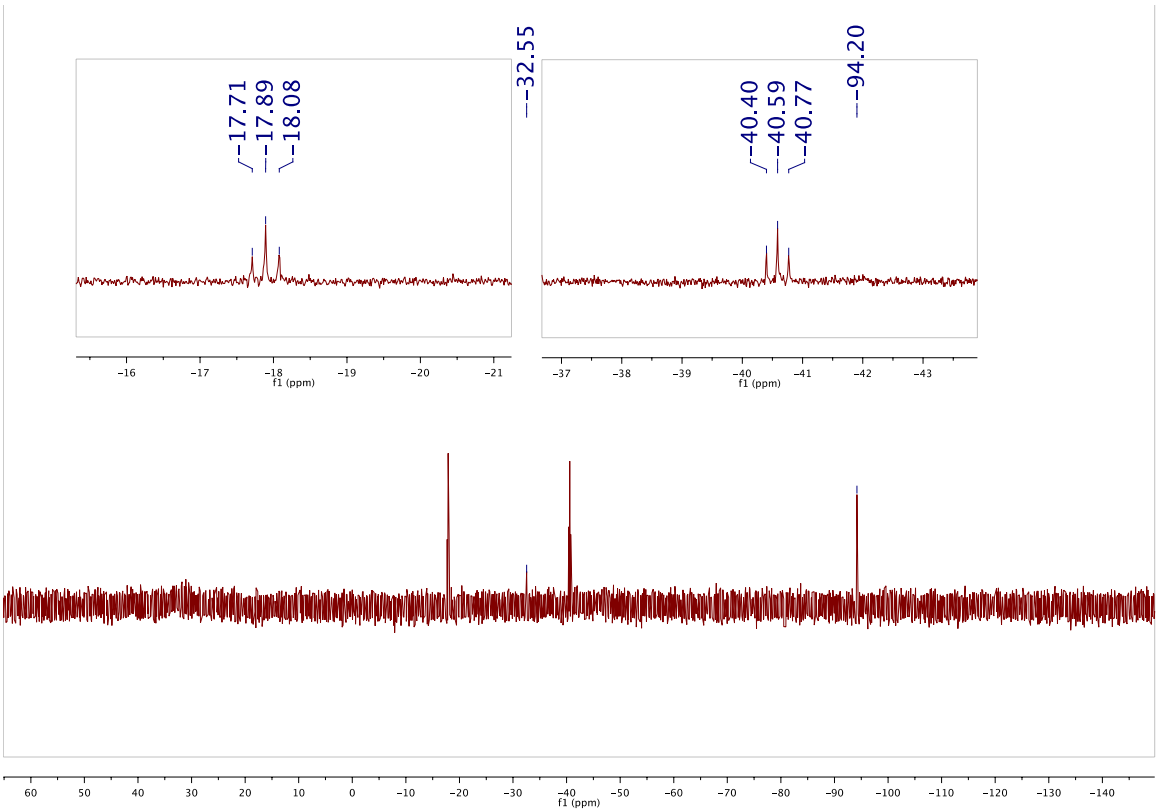
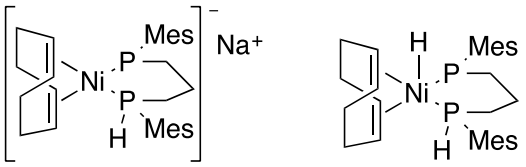


Chart 14. Resulting ^{31}P NMR spectrum of the attempted synthesis of the macrocycle through a bis-phosphido intermediate at room temperature (Scheme 16).



16 **17**

Scheme 15. Two possible single phosphido intermediates. **16** would result from deprotonation of the one of the donor phosphine atoms, while **17** would be the product of oxidative addition.

---

hydrophosphination reactions.[38] Such a transformation is observed using $Ni(COD)_2$ with secondary phosphine for the catalytic hydrophosphination of styrene[39] thus it would logical to infer that the presence of divinylphosphine promotes the formation of **17**.

In an effort to promote a bis-phosphido intermediate, the reaction was carried out at 70 ^{o}C. **14** was allowed to react for 24 hours without adding **4,** resulting in the total disappearance of the diastereomeric peaks and the appearance of a triplet at -47.0 ppm (Chart 16) consistent with phosphido species undergoing rapid inversion.[37]

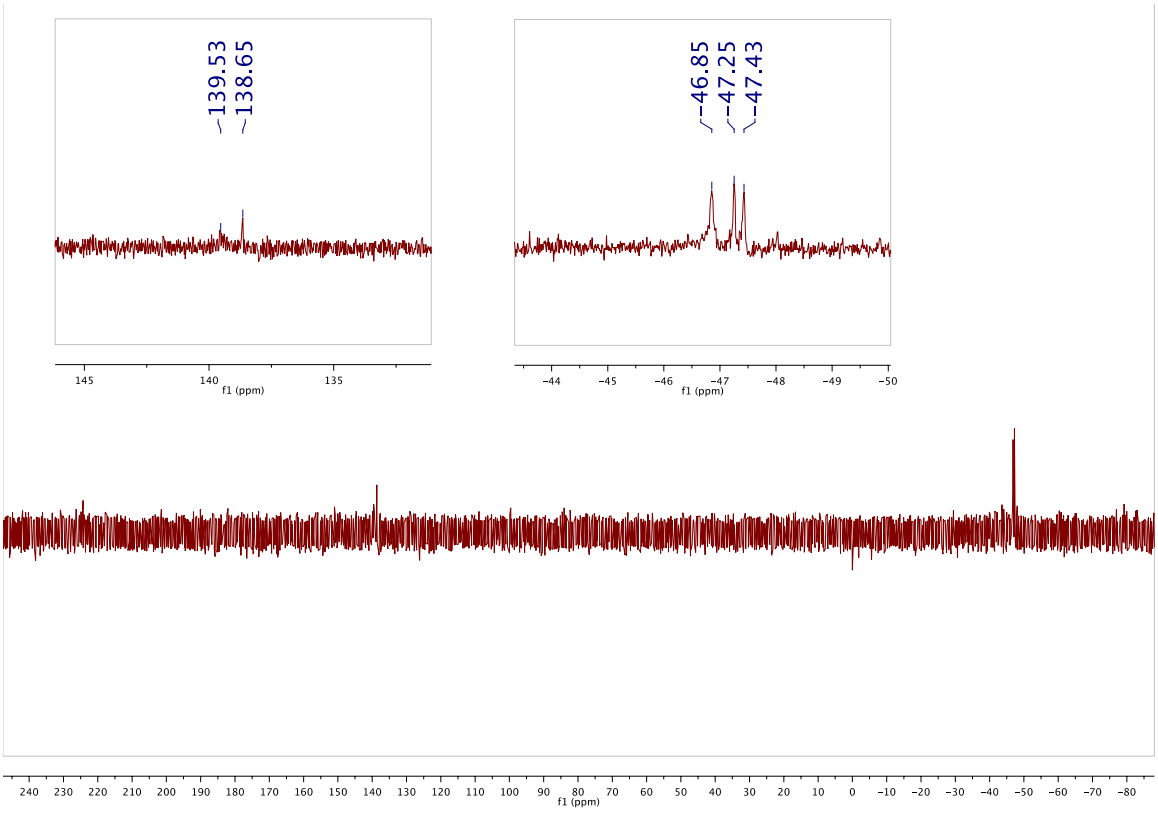
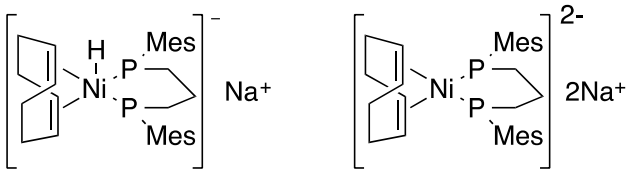


Chart 16. ^{31}P NMR spectra after reacting **14** with base for 24 hours at 70 ^{o}C. The chemical shift suggests the presence of a bis-phosphido intermediate.

As with the reaction at room temperature, the two most likely species (Chart 17) supported by this signal would be the result of double deprotonation **19** or oxidative addition **18**.



18 **19**

Chart 17. Possible bis-phosphido intermediates from oxidative addition, **18**, or double deprotonation, **19**.

An equivalent of **4** was added to this mixture resulting in multiplets at 100 ppm, -19.48 ppm, and -54.10 ppm. These signals, however are very faint, and cannot be interpreted easily. At time of writing, efforts to isolate these peaks are underway.

3. Conclusions

Though the target macrocycle was not reached with any certainty, the synthesis of the singly ligated complex serves as an important intermediate step towards that goal. The mesityl analogue of the bis-secondary phosphine ligand was synthesized over two synthetic steps from commercially available products with an overall yield of 20%. Use of the mesityl analogue proved to be the necessary synthetic pathway towards the macrocycle as it was able to coordinate to Ni(0) to form a stable singly ligated complex at room temperature, whereas the phenyl derivative generated only complex mixtures of isomers under a variety of conditions.

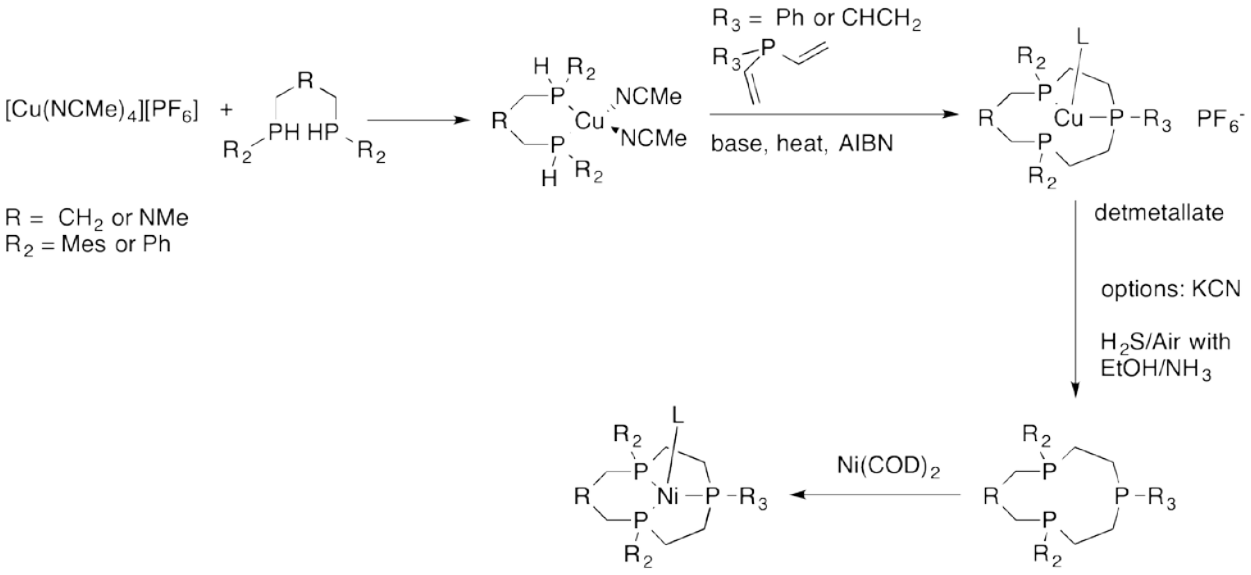
An interesting steric effect was discovered with the singly ligated complexes; only the *meso* isomer allows the coordination of moderately bulky ligands like $P(CHCH_2)_2Ph$. The *rac* isomer remains inactive. It was also shown that this steric effect can be circumvented by destroying the stereochemistry at the phosphine donor atoms bygeneration of the bis-phosphido intermediate. The stereoselectivity of the singly ligated complexes suggests that a radical initiated pathway (which begins by activation of the vinyl groups, rather than the phosphine

donor atoms) would likely be inefficient as only one isomer would be able to template the reaction. Thus, working through the phosphido intermediate represents a plausible path to the macrocycle, but the stereoslective coordination shown by the singly ligated complex suggests a route to tighter control over both steric and electronic environements of the catalyst, as well as a route to stereochemically diverse transition metal complexes.

4. Future Work

At this juncture it is clear that mesityl ligand is more suitable towards generation of the macrocycle; as such, further reactivity of the mesityl singly ligated complex (**13**) should be explored. Specifically, the ideal conditions for generating the phosphido intermediate (which is a very reactivity intermediate and easily quenched) should be investigated, including varying equivalents of base, temperature, time, and solvent. An AIBN catalyzed reaction should also be carried out with divinylphenylphosphine and the singly ligated complex to see if accessing the macrocycle through the phosphido intermediate is the preferred method.

Should the macrocycle still prove inaccessible, it may be pertinent to explore different template metals. The size of Ni(0)'s atomic radius may be inhibiting formation of the macrocycle; this inhibition could be alleviated by using Ni(II) instead. The obvious drawback of this approach as discussed in the introduction would be the necessity of EPR spectroscopy to characterize what would be paramagnetic complexes. Another approach that may alleviate both any restrictions due to the Ni(0)'s atomic radius and Ni's suspected role in catalyzing polymerization of the divinyl species would be to use Cu(I) as template, which have been shown to bind secondary bisphosphine ligands.[40] Cu(I) is diamagnetic and would enable characterization by NMR, however, Cu(I) is not catalytically prone to hydrogen activation. Thus this approach would necessitate demetallation of the macrocycle for coordination to a Ni species.



Scheme 17. Possible Cu(I) templated synthesis of the phosphine macrocycle.

In either case, once synthesis of the macrocyle complex is completed, its activity to bind or split dihydrogen should be explored. It would be pertinent to conduct electrochemical characterization of the complex and its active redox states to evaluate its potential as a molecular electrocatalyst through cyclic voltametery.

5. Experimental

Attempted Synthesis of (1,3-bis(phenylphosphino)propane)Ni(cyclooctadiene) (3)

i) 1 (40 mg, 0.145 mmol) was suspended in 1 mL of dry THF. A solution of **2** (38 mg, 0.145 mmol) in 1 mL of THF was added dropwise with stirring. An immediate color change was observed.

ii) 1 (40 mg, 0.145 mmol) was suspended in 1 mL of dry THF in schlenk flask flushed with nitrogen. Solution was cooled to -20^{o}C. A solution of **2** (38 mg, 0.145 mmol) in 1 mL of THF was also cooled to -20^{o}C and added dropwise via cannula transfer with stirring. Initially, a

yellow solution was observed, but underwent a color change to dark brown when warmed to room temperature.

$^{31}P\{^{1}H\}$NMR (THF, unlocked): δ 3.54 (d, J_{PP}= 14 Hz), 2.02 (s), -7.06 (t, J_{PP}= 14 Hz), -7.81 (s), -7.99 to -8.76 (m), -10.10 (s); Spectrum on S0

Attempted synthesis of (1,3-bis(phenylphosphino)propane)Ni(divinylphenylphosphine) (6)

1 (40 mg, 0.145 mmol) was suspended in 1 mL of dry THF. A solution of **4** (24 mg, 0.145 mmol) in 1 mL of THF was added dropwise with stirring. A yellow to orange color change was observed. The reaction mixture was allowed to stir for 20 hours, after which a solution of **2** (38 mg, 0.145 mmol) in 1 mL of THF was added; an immediate color from orange to dark brown was observed. $^{31}P\{^{1}H\}$NMR (THF, unlocked): δ 16.91 (s); Spectrum on S1

Attempted synthesis of (1,4,7-phenyl-1,4,7-triphosphacyclodecane)Ni (7)

1 (40 mg, 0.145 mmol) was suspended in 1 mL of dry THF with stirring in a Schlenk flask and cooled to -20 ^{o}C. In a separate flask, **4** (23.5 mg, 0.145 mmol) was dissolved in 1 mL dry THF and also cooled to -20 ^{o}C. After cooling, the solution of **4** was added dropwise to the solution of **1** via cannula and stirred for 1 hr at -20 ^{o}C. In a separate flask, **2** (38 mg, 0.145 mmol) was dissolved in THF, cooled to -20 ^{o}C, and subsequently added dropwise via cannula transfer to the reaction mixture. This mixture was allowed to stir for 45 minutes. In a separate flask, KOtBu (16.2 mg, 0.145 mmol) was suspended in 1 mL of THF, cooled to -20 ^{o}C, and added dropwise to the reaction mixture via cannula transfer. The reaction mixture was stirred overnight and allowed to reach room temperature. $^{31}P\{^{1}H\}$NMR (THF, unlocked): δ -7.08 (m), -7.84 (m), -10.15 (s); Spectrum on S2

Attempted synthesis of (1,4,7-phenyl-1,4,7-triphosphacyclodecane)Ni (7)

2 (38 mg, 0.145 mmol), **4** (23.5 mg, 0.145 mmol), and $P(C_6H_{11})_3$ (40.6 mg, 0.145 mmol) were dissolved in 3 mL of dry THF with stirring. In a separate vial, **1** (40 mg, 0.145 mmol) was suspended in 1 mL of dry THF and subsequently added dropwise the reaction mixture. Resulting orange solution allowed to stir for 24 hours. $NaOSiMe_3$ (32 mg, 0.290 mmol) was added to the reaction mixture and allowed to stir for 48 hours.

Before addition of base; $^{31}P\{^1H\}$NMR (THF, unlocked): δ 21.57 (t, J_{PP}=14 Hz), 10.91 (s), -7.06 (t, J_{PP}= 24 Hz), -7.81 (s), -7.85 (m), -10.10 (s), -11.42 (t, J_{PP}= 17 Hz), -12.14 (t, J= 17 Hz), -15.23 (s); Spectrum on S3

After addition of base; $^{31}P\{^1H\}$NMR (THF, unlocked): δ -10.97 (s), -7.19 (s), -7.77 (s), -15.13 (m); Spectrum on S4

Synthesis of Mesitylphosphonous dichloride (9) 8 (4.9 g, 25 mmol) was degassed under vacuum in a schlenk flask, then dissolved in 100 mL of dry THF under nitrogen. The solution was cooled to -30^oC and nBuLi (13.75 mL of a 2 M solution, 27.5 mmol) was added via cannula transfer. The reaction mixture was allowed to stir for 2 hours. A solution of phosphorus trichloride (3.78 g, 27.5 mmol) in 10 mL of THF prepared and added to reaction mixture via cannula transfer. The reaction mixture was stirred overnight. A Product peak was observed by ^{31}PNMR and taken forward without further purification. $^{31}P\{^1H\}$NMR (THF, unlocked): 169.33

Synthesis of Mesitylphosphine (10) The reaction mixture of the previous step was cooled to 0^oC and transferred via cannula to a schlenk flask flushed with nitrogen containing LAH (1.91 g, 50 mmol). The reaction mixture was stirred overnight, and subsequently quenched with 60 mL of degassed 20% HCL solution via slow cannula transfer. The THF layer was collected and the remaining aqueous layer was extracted two times with 50 mL of diethyl ether. The organic

extract was dried over magnesium sulfate, filtered, then evaporated under reduced pressure. The resulting oil was purified by kueglrohr distillation; the product condensed at 100^{o}C under 0.94 torr affording **10** (2.58 g) as a clear oil in 67.7% yield. ^{31}P NMR(C_6D_6): δ -155.32 (t, J_{PH}= 201, P-H)

This chemical shift agrees with published values. Decoupled spectrum on S5, coupled spectrum on S6

Synthesis of 1,3-bis(mesitylphosphino)propane (12) 10 (1 g, 6.57 mmol) was dissolved in 75 mL of dry DMSO under nitrogen. Freshly ground KOH (380 mg, 6.57 mmol) was added to the solution with stirring. The yellow reaction mixture was allowed to stir for 3 hours. **11** (0.31 mL, 0.328 mmol) was added via syringe. The reaction mixture was allowed to stir for 4 hours until clear and was quenched with 60 mL degassed water. The solution was extracted three times with 60 mL diethyl ether. The organic extract was dried with magnesium sulfate, then filtered and evaporated. The resulting oil was purified by kugelrhor distillation at 0.94 torr. Impurities boiled off around 150 ^{o}C to afford **12** as a white solid (0.659 g) in 29% yield. ^{31}P NMR(C_6D_6): δ -87.0 (d, J_{PH} =214, P-H), -87.2 (d, J_{PH}= 214, P-H).

These chemical shifts agree with published values

Impurity at -92.7, Spectrum on S7, coupled spectrum on S8

Synthesis of (1,3-bis(mesitylphosphino)propane)Ni(cyclooctadiene) (13) 1 (25 mg, 0.09 mmol) was suspended in 1 mL of dry THF. A solution of **12** (31 mg, 0.09 mmol) in 1 mL of THF was added dropwise with stirring. A gradual color change from yellow to a dark, rust color was observed. ^{31}P{^{1}H}NMR (THF, unlocked): δ -20.64 (s), -25.44 (s); Spectrum on S9

Attempted synthesis of *meso* (1,3-bis(mesitylphosphino)propane) Ni(phenyldivinylphosphine) (14) 1 (25 mg, 0.09 mmol) was suspended in 1 mL of dry THF. A

solution of **12** (31 mg, 0.09 mmol) in 1 mL of THF was added dropwise with stirring. The mixture was allowed to stir at room temperature for 1 hour. In a separate vial, **4** (14 mg, 0.09 mmol) was dissolved in 1 mL of THF and added dropwise to the reaction mixture. $^{31}P\{^{1}H\}$NMR (THF, unlocked): δ 6.58 (s), -21.40 (s), -26.20 (s), -32.05 (s), -38.08 (d, J_{PP}= 58 Hz), -39.97 (d. J_{PP}= 38 Hz), -44.38 (d, J_{PP}= 58 Hz); Spectrum on S10

Attempted Synthesis of (1,7-mesityl-4-phenyl-1,4,7-triphosphacyclodecane) (15)

i) 1 (25 mg, 0.09 mmol) was suspended in 1 mL of dry THF. A solution of **12** (31 mg, 0.09 mmol) in 1 mL of THF was added dropwise with stirring. This mixture was allowed to stir for 30 minutes. $NaOSiMe_3$ (20.2 mg, 0.18 mmol) was added to reaction mixture and stirred for 1 hour. A solution of **4** in 1 mL of THF was added to the reaction mixture. A portion of this mixture was moved to a sealed NMR tube and heated at 70 ^{o}C for 48 hours. The remainder of the mixture was stirred at room temperature for 48 hours. $^{31}P\{^{1}H\}$NMR (THF, unlocked): δ -17.89 (t, J_{PP}= 30 Hz), -40.59 (t, J_{PP}= 30 Hz)**;** Spectrum on S11

ii) 1 (25 mg, 0.09 mmol) was suspended in 1 mL of dry THF. A solution of **12** (31 mg, 0.09 mmol) in 1 mL of THF was added dropwise with stirring. This mixture was allowed to stir for 1 hour. $NaOSiMe_3$ (20.2 mg, 0.18 mmol) was added to reaction mixture. Reaction mixture was moved to a sealed NMR tube and heated at 70 ^{o}C for 26 hours. Solution of **4** (14 mg, 0.09 mmol) was added to the mixture and heated for 16 hours at 70 ^{o}C.

Before addition of **4:** $^{31}P\{^{1}H\}$NMR (THF, unlocked): δ 138.65 (m), -47.26 (t, J_{PP}= 30 Hz); Spectrum on S12

After addition of **4:** $^{31}P\{^{1}H\}$NMR (THF, unlocked): δ 100 (m), -19.48 (m), -54.10; Spectrum on S13

6. References:

1. Energy Information Administration. International Energy Outlook 2013. http://www.eia.gov/forecasts/ieo/ (accessed Oct. 22, 2014).

2. Energy Information Administration. Energy Explained: Greenhouse Gases Effect on Climate. http://www.eia.gov/energyexplained/index.cfm?page=environment_how_ghg_affect_climate (accessed Oct. 22, 2014).

3. Evans, D. J.; Pickett, C. J. Chemistry and the Hydrogenases. *Chem. Soc. Rev.* **2003**. 32, 268-275

4. Jones, A. K.; Sillery, E.; Albracht, S. P. J.; Armstrong, F. A. Direct Comparison of the Electrocatalytic Oxidation of Hydrogen by an Enzyme and Platinum Catalyst. *Chem. Comm.* **2002**. 866-867.

5. Tard, C.; Pickett, C. Structural and Functional Analogues of the Active Sites of the [Fe]-, [NiFe]-, and [FeFe]-Hydrogenases. *Chem. Rev.* **2009.** 109, 2245-2274.

6. Lubitz, W.; Ogata, H.; Rudiger, O.; Reijerse, E. Hydrogenases. *Chem. Rev*. **2014.** 114, 4081-4181.

7. Krasna, A. I. Hydrogenase: Properties and Applications. *Enzyme Microb. Technol*. **1979**, 1, 165-172.

8. Esswein, A. J.; Nocera, D. G.; Hydrogen Production by Molecular Photocatalysis. *Chem. Rev.* **2007**. 107, 4022-4047.

9. Yang, X.; Hall, M. B. Monoiron Hydrogenase Catalysis: Hydrogen Activation with the Formation of a Dihydrogen, Fe-H^(δ-)···H^(δ+)-O, Bond and Methenyl-H_4MPT^+ Triggered Hydride Transfer. *J. Am. Chem. Soc.* **2009**. 131, 10901-10908.

10. Ogata, H.; Hirota, S.; Nakahara, A.; Komori, H.; Shibata, N.; Kato, T.; Kano, K.; Higuchi, Y. Activation Process of [NiFe] Hydrogenase Elucidated by High-Resolution X-Ray Analyses: Conversion of the Ready to the Unready State. *Structure.* **2005**. 13, 1635-1642.

11. Nicolet, Y.; Prias, C.; Legrand, P.; Hatchikian, C. E.; Fontecilla-Camps, J. C. Desulfovibrio desulfuricans Iron Hydrogenase: the Structure Shows Unusual Coordination to an Active Site Fe Binuclear Center. *Structure*. **1999**. 7, 13-23.

12. Roy, S.; Mazinai, S. K. S.; Groy, T. L.; Gan, L.; Tarakeshwar, P.; Mujica, V.; Jones, K. A. Catalytic Hydrogen Evolution by Fe(II) Carbonyls Featuring a Dithiolate and a Chelating Phosphine. *Inorg. Chem.* **2014**. 8919-8929.

13. Chambers, G. M.; Angamuthu, R.; Gray, D. L.; Rauchfuss, T. B. Organo Ruthenium-Nickel Dithiolates with Redox-Responsive Nickel Sites. *Organometallics.* **2013**. 66324-6329.

14. Ohki, Y.; Yasumura, K.; Ando, M.; Shimokata, S.; Tatsumi, K. A Model for the CO-inhibited Form of [NiFe] Hydrogenase: Synthesis of $(CO)_3Fe(\mu\text{-}S^tBu)_3Ni\{SC_6H_3\text{-}2,6\text{-}(mesityl)_2\}$ and reversible CO addition at the Ni site. **2010.** 3994-3997.

15. Carroll, M. E.; Barton, B. E.; Rauchfuss, T. B.; Carroll, P. J. Synthetic Models for the Active Site of the [FeFe]-Hydrogenase: Catalytic Proton Reduction and the Structure of the Doubly Protonated Intermediate. *J. Am. Chem. Soc.* **2012**. 134, 18843-18852.

16. Liu, T.; Chen, S.; O'Hagan, M. J.; DuBois, M. R.; Bullock, R. M.; DuBois, D. L. Synthesis, Characterization, and Reactivity of Fe Complexes Containing Cyclic Diazadiphosphine Ligands: The Role of the Pendant Base in Heterolytic Cleavage of H_2. *J. Am. Chem. Soc.* **2012**. 134, 6257-6272.

17. Rountree, E. S.; McCarthy, B. D.; Eisenhart, T. T.; Dempsey, J. L. Evaluation of Homogeneous Electrocatalysts by Cyclic Voltammetry. *Inorg. Chem.* **2014**. 53, 9983-10002.

18. Helm, M. L.; Stewart, M. P.; Bullock, R. M.; DuBois, M. R.; DuBois, D. L. A Synthetic Nickel Electrocatalyst with a Turnover Frequency Above 100,000 s^{-1} for H_2 Production. *Science.* **2011**. 333, 863-866.

19. Liu, T.; DuBois, D. L.; Bullock, R. M. An Iron Complex with Pendent Amines as a Molecular Electrocatalyst for Oxidation of Hydrogen. *Nature Chem.* **2013**. 5. 228-233.

20. O'Hagan, M.; Ho, M.; Yang, J.; Appel, A. M.; DuBois, M. R.; Raugei, S.; Shaw, W. J.; DuBois, D. L.; Bullock, R. M. Proton Delivery and Removal in $[Ni(P^{R}_{2}N^{R'}_{2})_2]^{2+}$ Hydrogen Production and Oxidation Catalysts. *J. Am. Chem. Soc.* **2012**. 134. 19409-19424.

21. Leeuwen, P. W. N .M.; Kamer, P. C. J.; Reek, J. N. H.; Dierkes, P. Ligand Bite Angle Effects in Metal-catalyzed C-C Bond Formation. *Chem. Rev.* **2000**. 100, 2741-2769.

22. Edwards, P. G.; Haigh, R.; Li, D.; Newman, P. D. Template Synthesis of 1,4,7 Triphosphacyclononane. *J. Am. Chem. Soc.* **2006**. 128. 3818-3830.

23. Edwards, P. G.; Malik, K. M. A.; Ooi, L.; Price, A. J. Iron Complexes of Facially Capping Triphosphorus Macrocycles. *Dalton Trans.* **2006**. 433-441.

24. Battle, A. R.; Edwards, P. G.; Haigh, R.; Hibbs, D. E.; Li, D. Liddiard, S. M.; Newman, P. D. Synthesis and Characterization of Iron (II) Complexes of 10- and 11-Membered Triphosphamacrocycles. *Organometallics.* **2007**. 26, 377-386.

25. Diel, B. N.; Brandt, P. F.; Haltiwanger, R. C.; Norman, A. D. Metal-templated Synthesis of Macrocyclic Triphosphine-Molybdenum Complex, Fac-$(CO)_3Mo(PHC_3H_6)$ *J. Am. Chem. Soc.* **1982**, 104, 4700.

26. Brauer, D. J.; Lebbe, T.; Stelzer, O. Template Synthesis of Macrocyclic Multiphosphane Ligands with Functional Groups. *Angew. Chem. Int. Ed.* **1988**. 27, 438-439.

27. Pascariu, A.; Iliescu, S.; Popa, A.; Ilia, G. Polydentate Phosphines *J. Organometallic Chem.* **2009**. 694, 3982-4000.

28. Karasik, A. A.; Naumov, R. N.; Spiridonova, Y. S.; Sinyashin, O. G.; Lonnecke, P.; Hey-Hawkins, E. Synthesis, Molecular Structure and Coordination Chemistry of the First 1-Aza-3,7-diphosphacyclooctanes. *Z. Anorg. Allg. Chem.* **2007**. 205-210.

29. Monkowius, U.; Nogai, S.; Schmidbaur, H. Contributions to the Little Known Chemistry of Trivinylphosphine and Trivinylarsine. *Organometallics.* **2003**. 22, 145-152.

30. Sterzik, A.; Lonnecke, P.; Hey-Hawkins, E. Secondary Hydroxyalkylphosphanes: Synthesis and Characterization of Mono-, Bis- and Trialkoxyphosphane-substituted Zirconium Complexes and the Heterobimetallic Trinuclear Complex $[Cp_2Zr\{O(CH_2)_3PHMes(AuCl)\}_2]$. *Z. Anorg. Allg. Chem.* **2005.** 631, 2457-2466.

31. Curtis, C. J; Medaner, A.; Clancanelli, R.; Ellis, W. W.; Noll, B. C.; DuBois, M. R.; DuBois, D. L. $[Ni(Et_2PCH_2NMeCH_2Pet_2)_2]^{2+}$ as a Functional Model for Hydrogenases. *Inorg Chem.* **2003**. 42, 216-227.

32. Bonrath, W.; Porschke, K. R.; Wilke, G.; Angermund, K.; Kruger, C. Mono- and Dinculear Nickel(0) Complexes of Butadiyne. *Angew. Chem. Int. Ed.* **1988**. 27, 833-835.

33. Lowry, D. J.; Helm, M. L. Synthesis of 1,4,7-Triphenyl-1,4,7-triphsophacyclononane: The First Metal-Free Synthesis of a [9]-aneP_3R_3 Ring. *Inorg. Chem.* **2010,** 49, 4732-4734.

34. Shannon, R. D. Revised Effective Ionic Radii and Systematic Studies of Interatomic Distances in Halides and Chalocgenides. *Acta Crystallogr*. **1976**, A32, 751-767

35. Deming, J. T.; Novak, M. B.; Preparation and Reactivity Studies of Highly Versatile Nickel-Based Catalyst Systems. *Macromolecules.* **1993**, 26, 7089-7091.

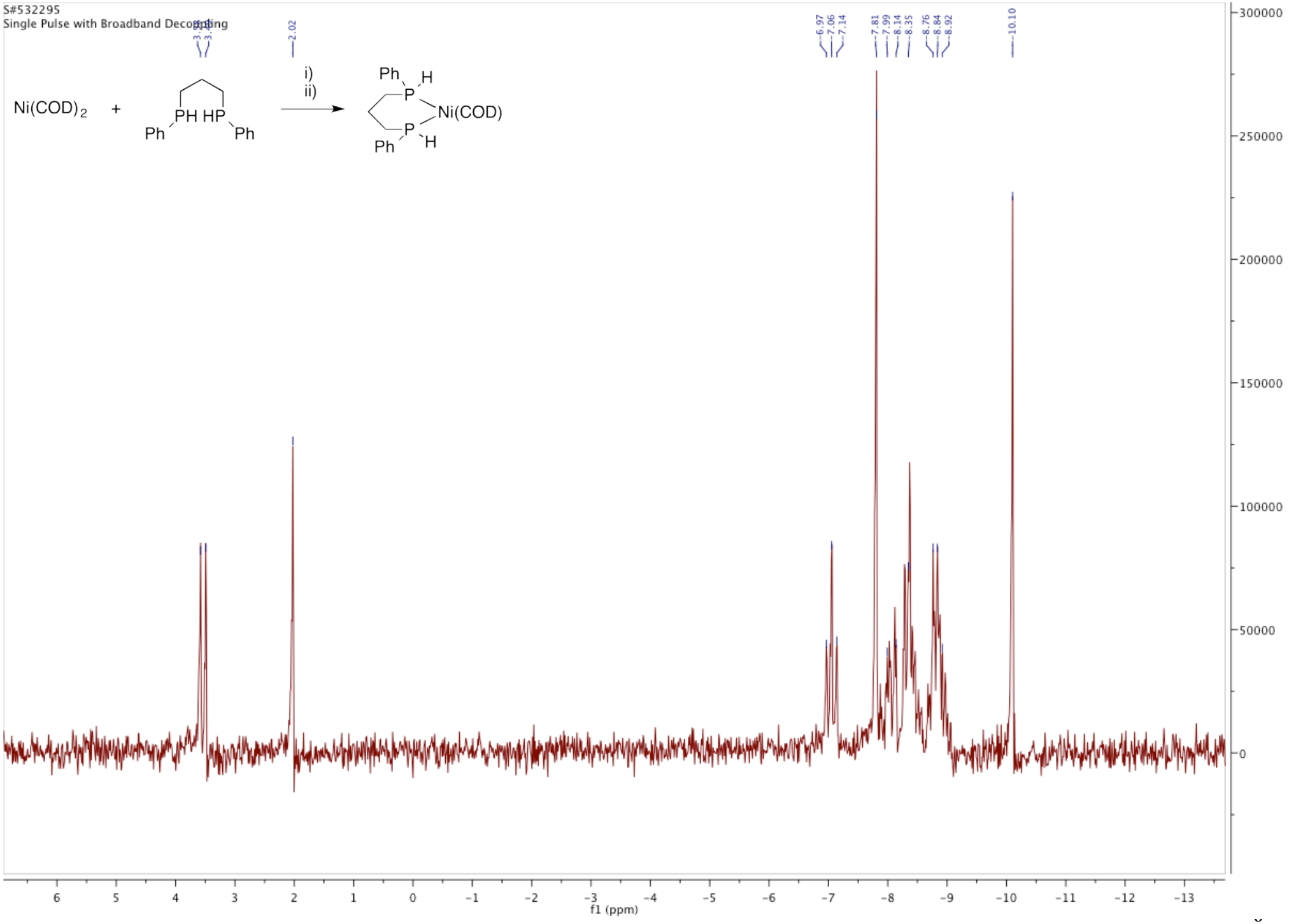
36. Wang, C.; Friedrich, S.; Younkin, T. R.; Li, R. T.; Grubbs, R. H.; Bansleben, D. A.; Day, M. W. Neutral Nickel(II)-Based Catalysts for Ethylene Polymerization. *Organometallics.* **1998.** 17, 3149-3151.

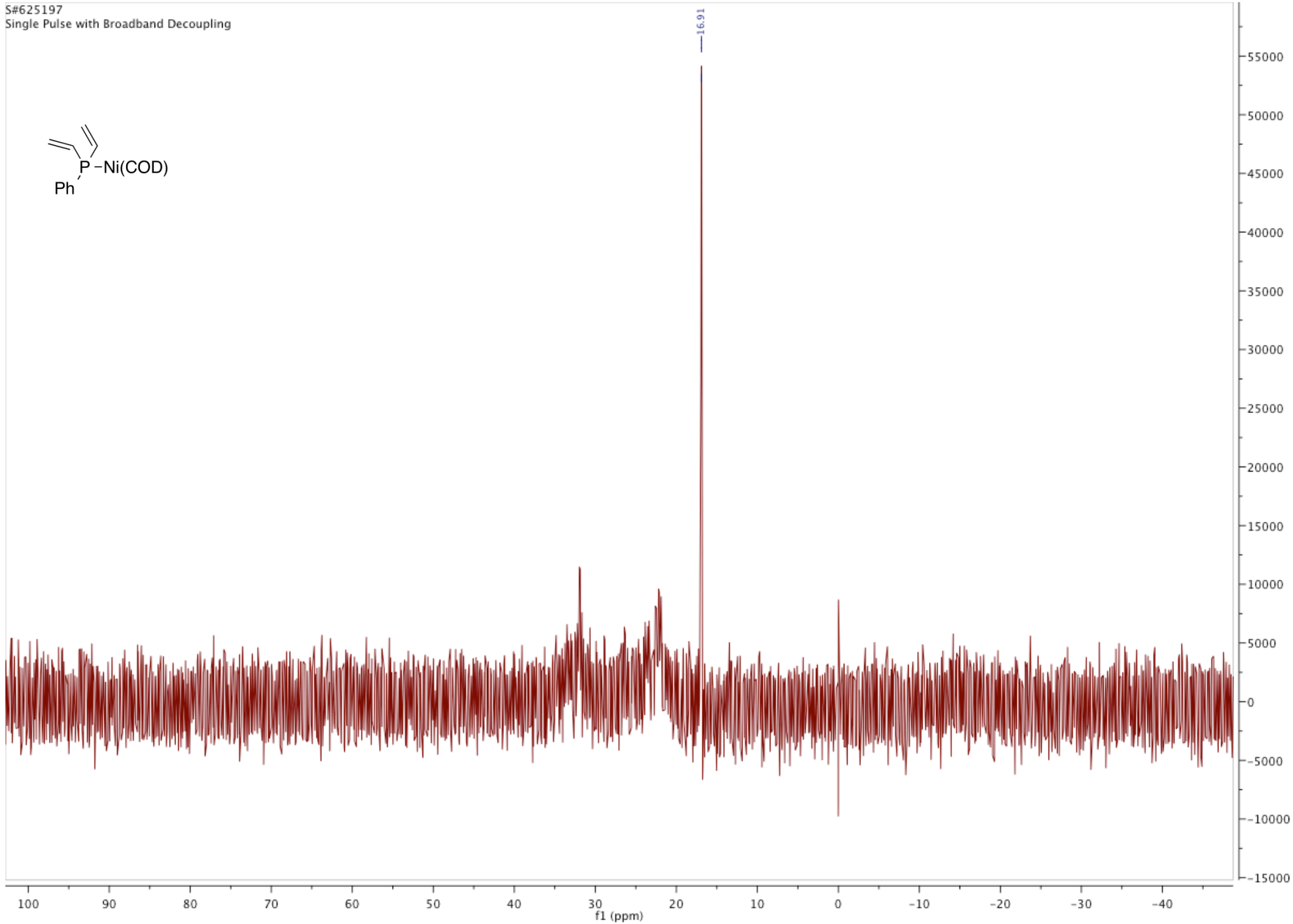
37. Scriban, C.; Wicht, D. K.; Glueck, D. S.; Zakharov, L. N.; Golen, J. A.; Rheingold, A. L. Platinum (II) Phosphiodo Complexes as Metalloligands. Structural and Spectrscopic Consequences of Conversion from Terminal to Bridging Coordination. *Organometallics.* **2006**, 25, 3370-3378.

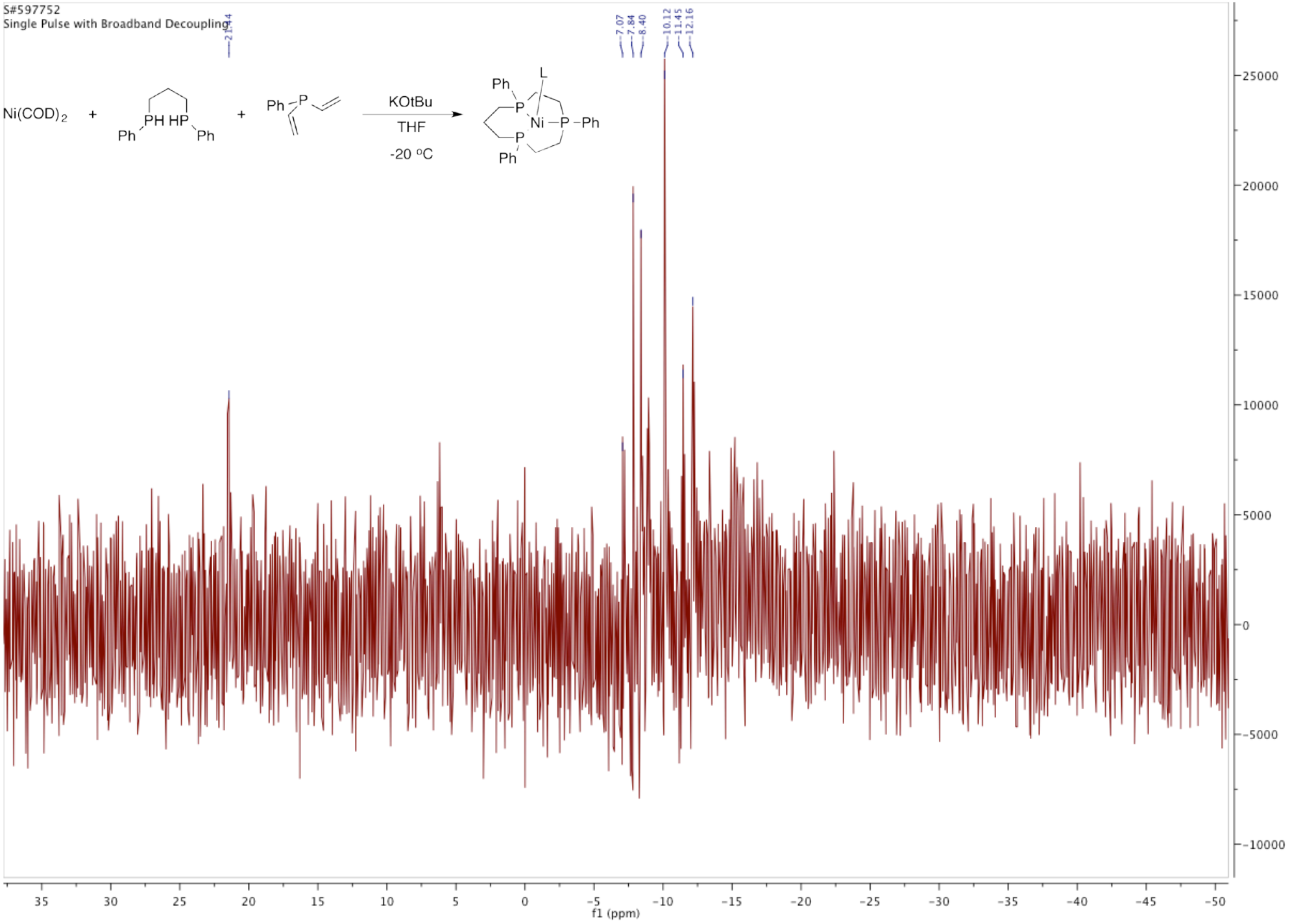
38. Rosenberg, L. Mechanisms of Metal-Catalyzed Hydrophosphination of Alkenes and Alkynes. *ACS Catal.* **2013**. 3, 2845-2855.

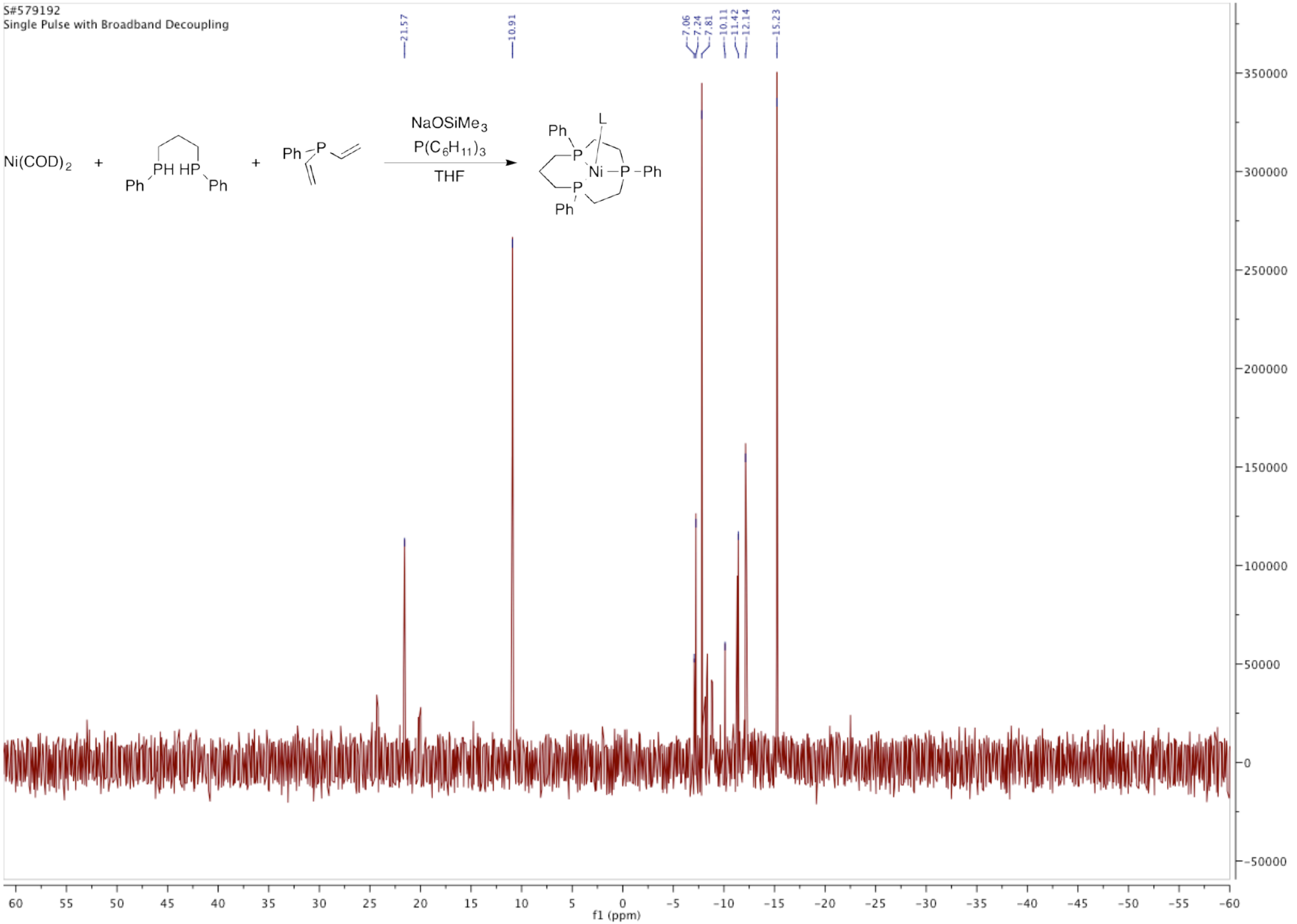
39. Shulyupin, M. O.; Kazankova, M. A.; Beletskaya, I. P. Catalytic Hydrophosphination of Styrenes. *Org. Lett.* **2002**. 4, 761-763.

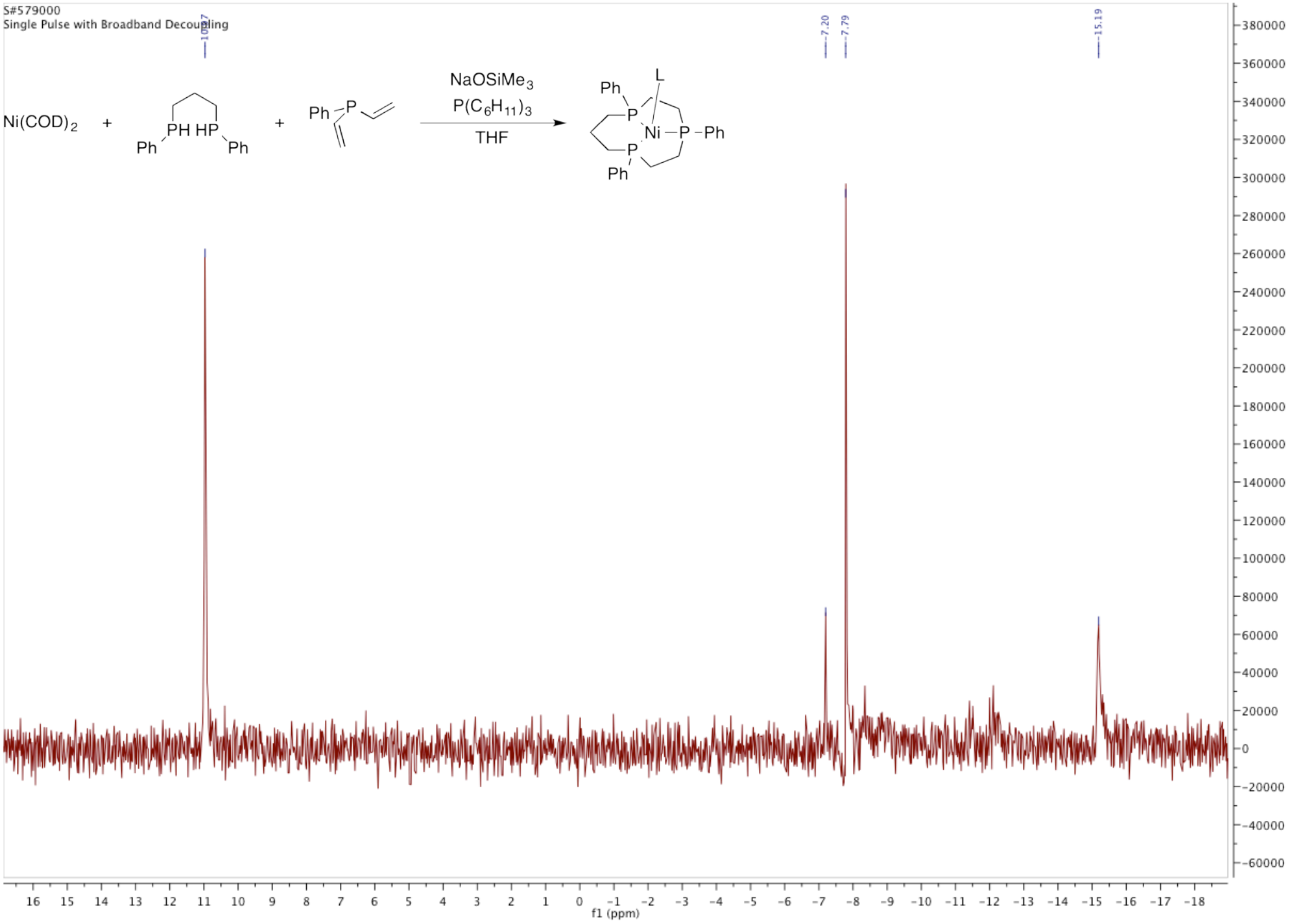
40. Doel, L. C.; Gibson, A. M.; Reid, G. Synthesis and Multinuclear NMR Studies On Copper and Silver Complexes of Multidentate Phosphine and Mixed Phospha.Thia Ligands. Single Crystal Structure of $[Cu(P_2S_2)]PF_6$ (P_2S_2= $Ph_2PCH_2SCH_2CH_2PPh_2$). *Polyhedron*. **1995**. 14, 3139-3146.

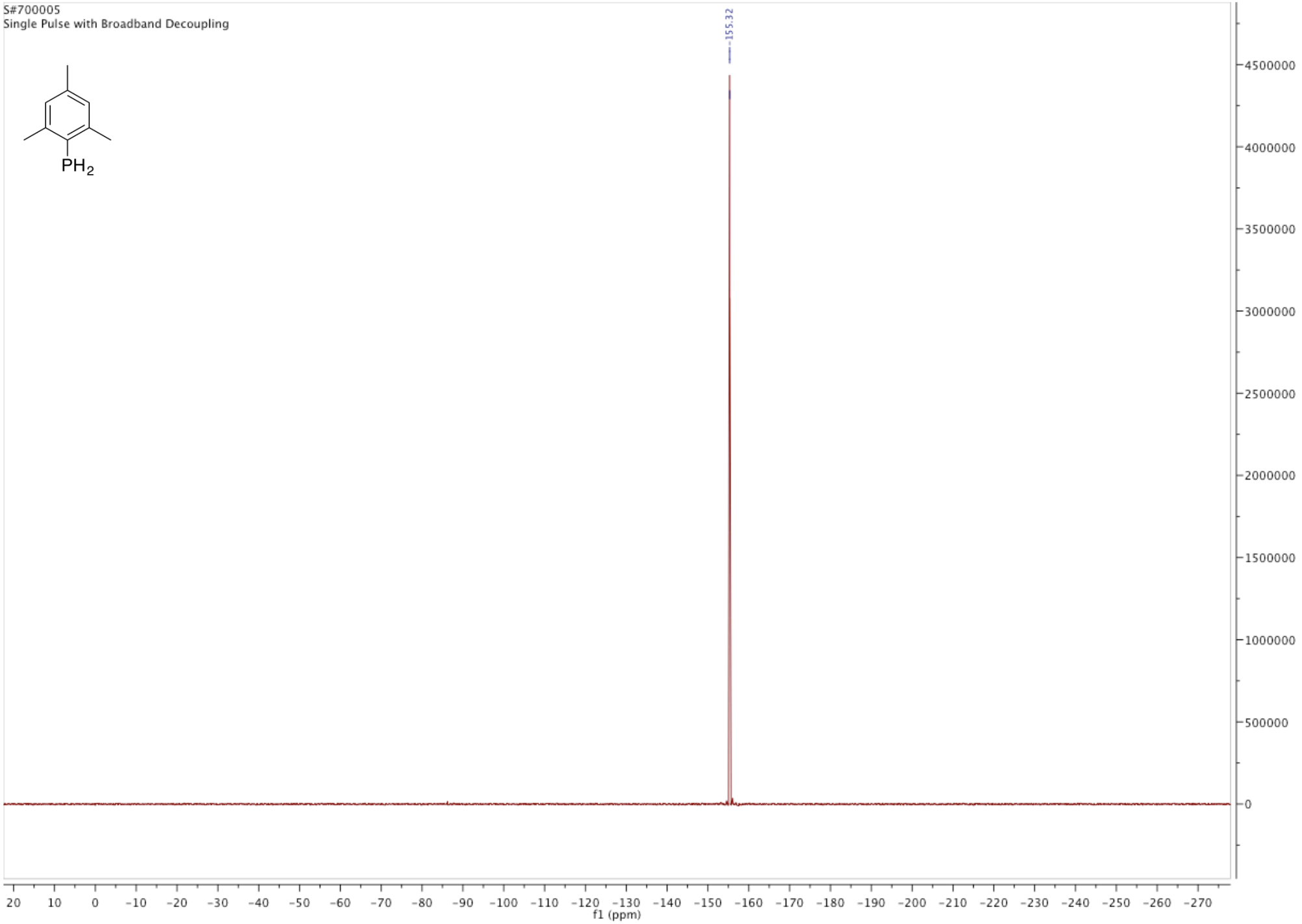

S#532295
Single Pulse with Broadband Decoupling
3.34
3.31
2.02
6.97
7.06
7.14
7.81
7.99
8.14
8.35
8.76
8.84
8.92
10.10
Ni(COD)2
+
PH HP
Ph
Ph
i)
ii)
Ph
H
P
Ni(COD)
P
Ph
H
300000
250000
200000
150000
100000
50000
0
6
5
4
3
2
1
0
−1
−2
−3
−4
−5
−6
−7
−8
−9
−10
−11
−12
−13
f1 (ppm)

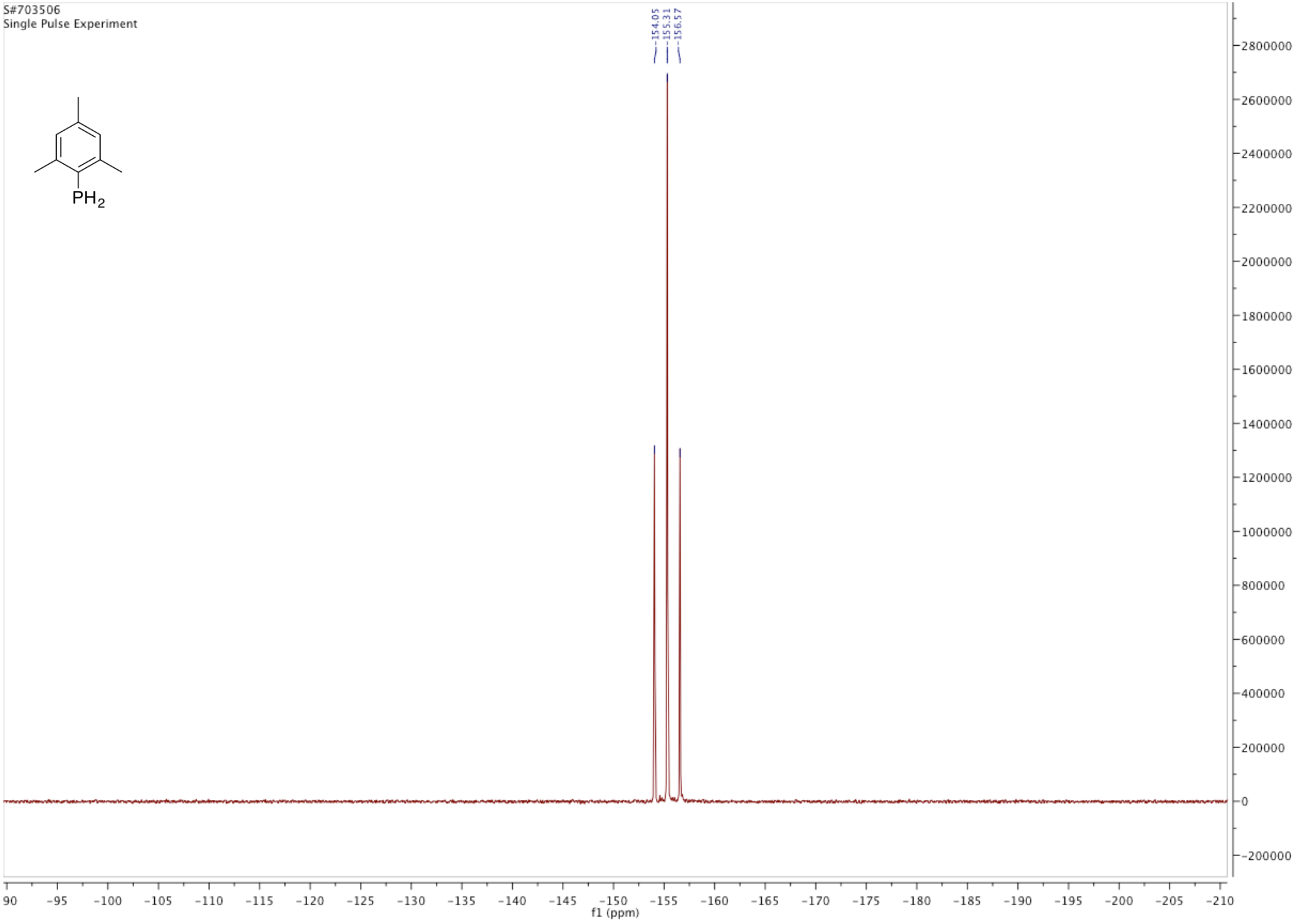

S#625197
Single Pulse with Broadband Decoupling
16.91
P
Ni(COD)
Ph
55000
50000
45000
40000
35000
30000
25000
20000
15000
10000
5000
0
-5000
-10000
-15000
100
90
80
70
60
50
40
30
20
10
0
-10
-20
-30
-40
f1 (ppm)

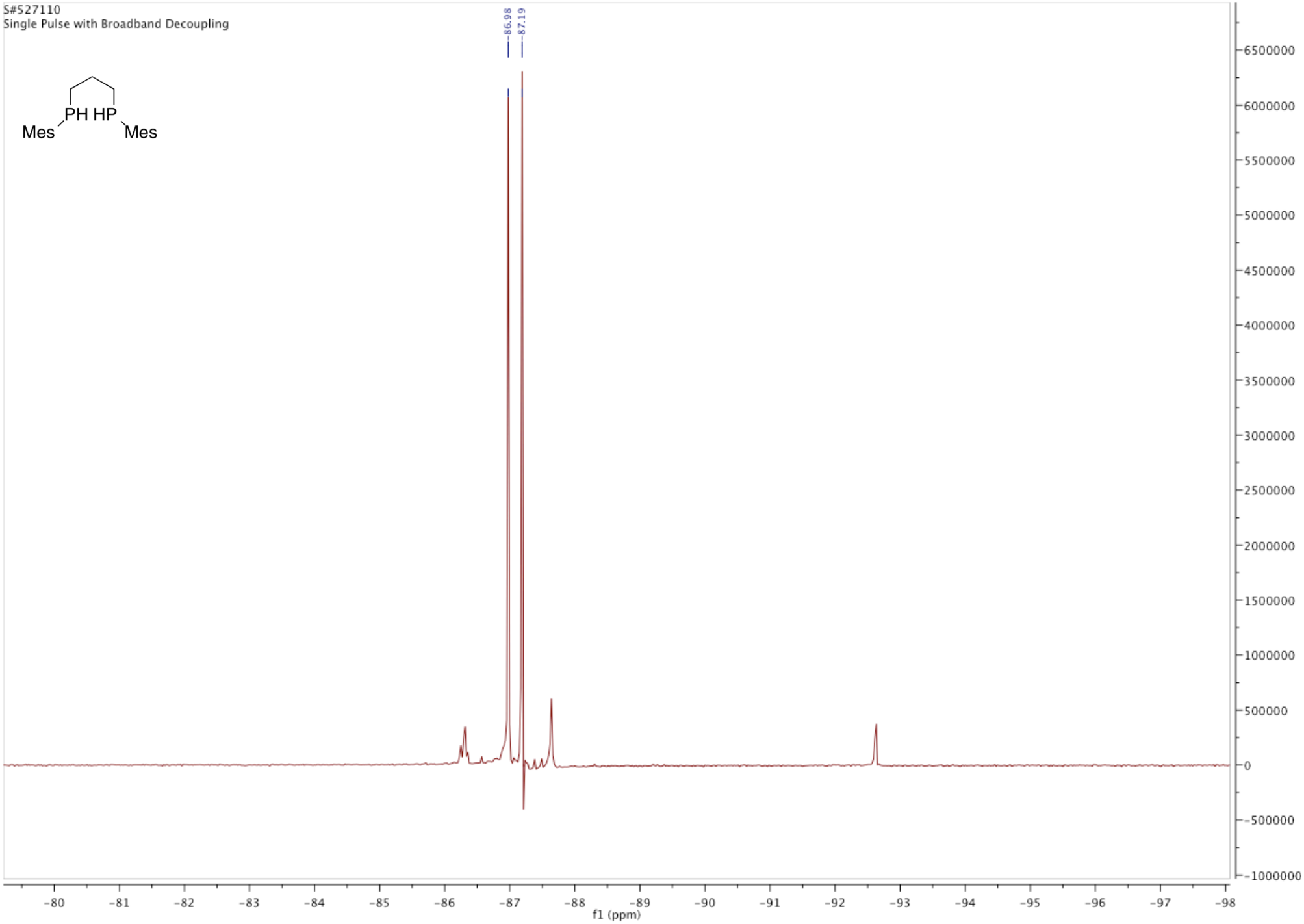

S#597752
Single Pulse with Broadband Decoupling
Ni(COD)2
PH HP
Ph
Ph
P
KOtBu
THF
-20 °C
L
Ni
7.07
7.84
8.40
10.12
11.45
12.16
25000
20000
15000
10000
5000
0
-5000
-10000
35
30
25
20
15
10
5
0
-5
-10
-15
-20
-25
-30
-35
-40
-45
-50
f1 (ppm)

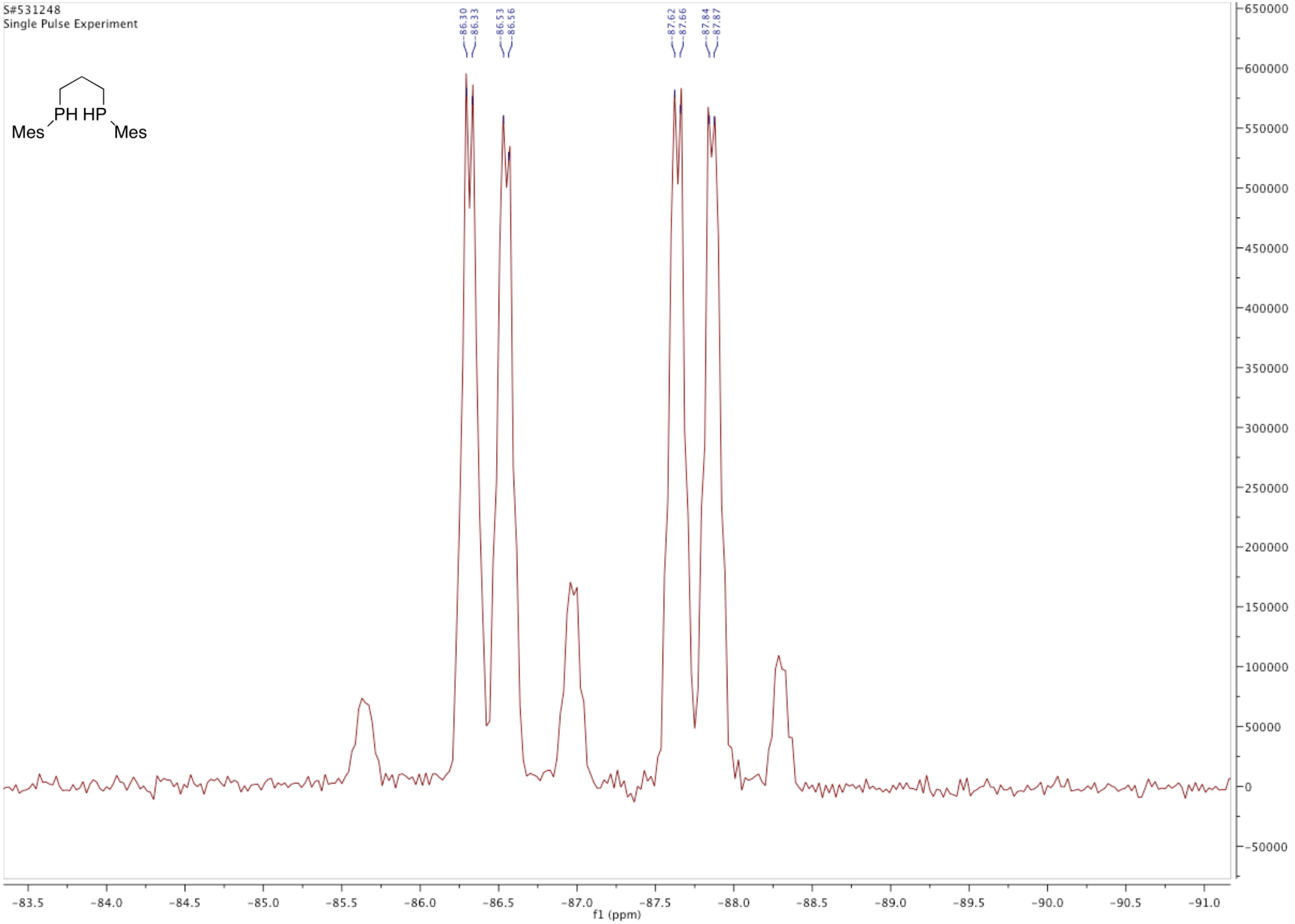

S#579192
Single Pulse with Broadband Decoupling
21.57
10.91
7.06
7.24
7.81
10.11
11.42
12.14
15.23
Ni(COD)2
PH HP
Ph
Ph
Ph
P
NaOSiMe3
P(C6H11)3
THF
L
Ni
f1 (ppm)

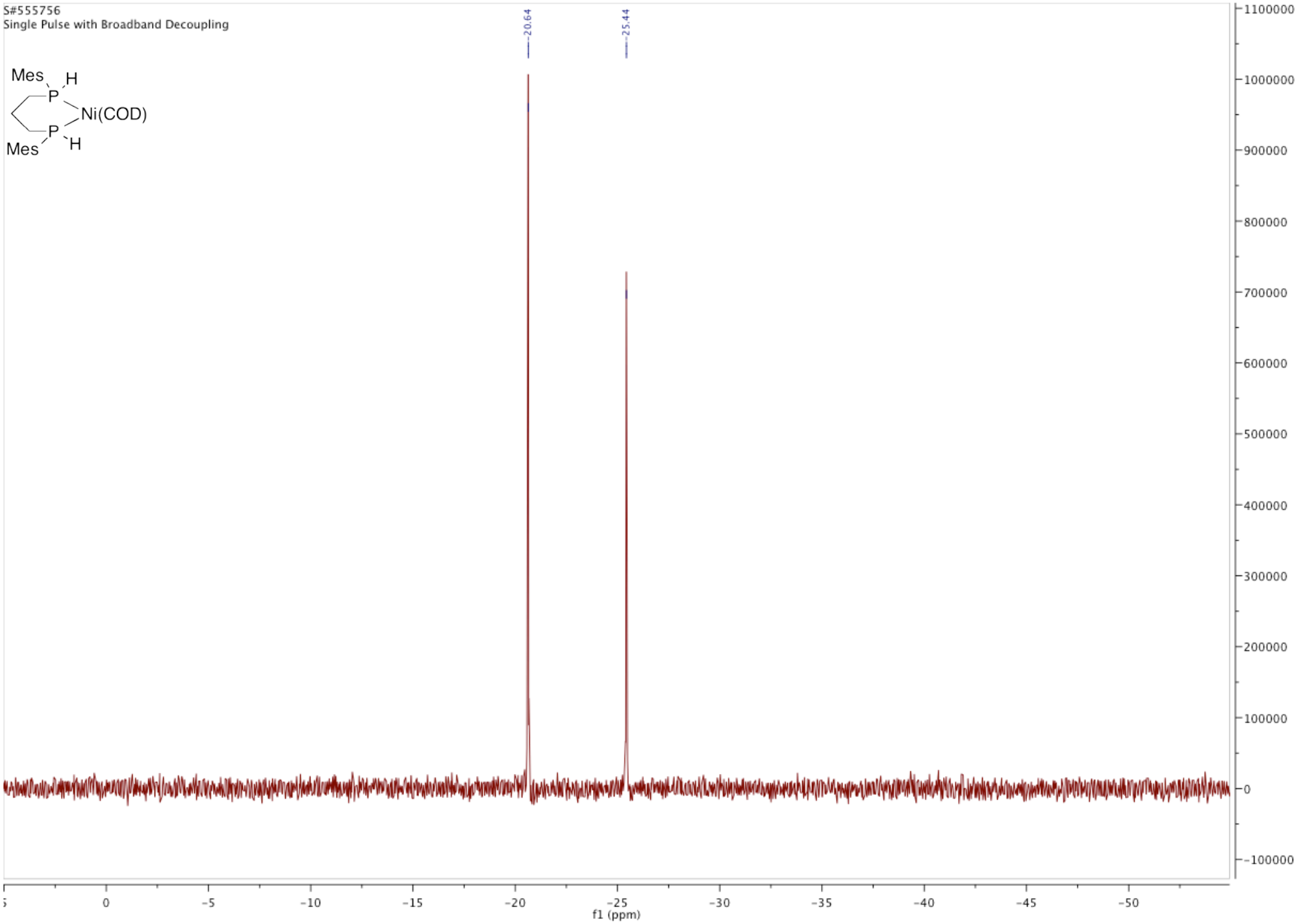

S#579000
Single Pulse with Broadband Decoupling
11.07
7.20
7.79
15.19
Ni(COD)2
+
PH HP
Ph
Ph
+
Ph
P
NaOSiMe3
P(C6H11)3
THF
L
Ph
P
Ni
P
Ph
P
Ph
f1 (ppm)

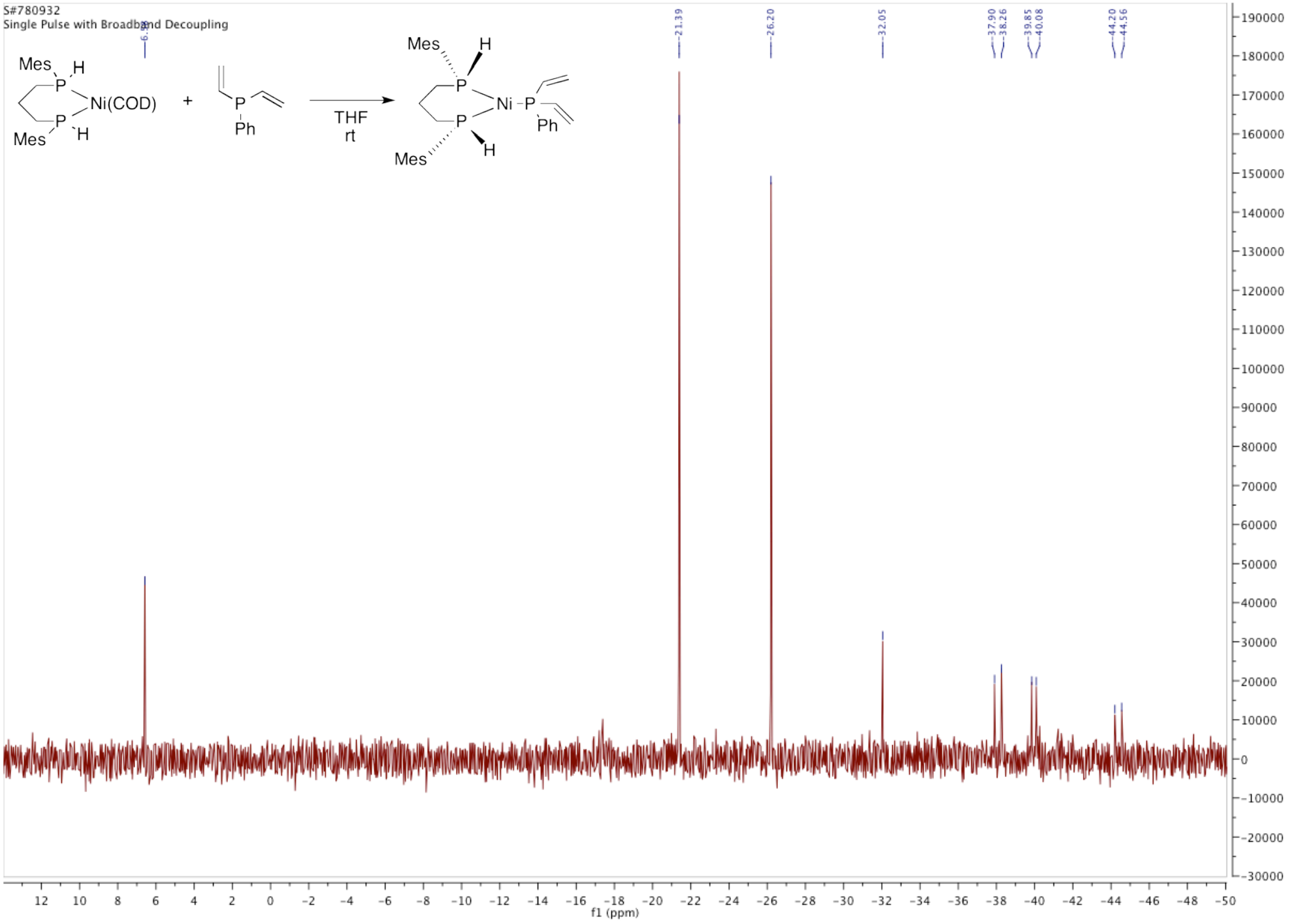

S#700005
Single Pulse with Broadband Decoupling
155.32
PH2
4500000
4000000
3500000
3000000
2500000
2000000
1500000
1000000
500000
0
20 10 0 -10 -20 -30 -40 -50 -60 -70 -80 -90 -100 -110 -120 -130 -140 -150 -160 -170 -180 -190 -200 -210 -220 -230 -240 -250 -260 -270
f1 (ppm)

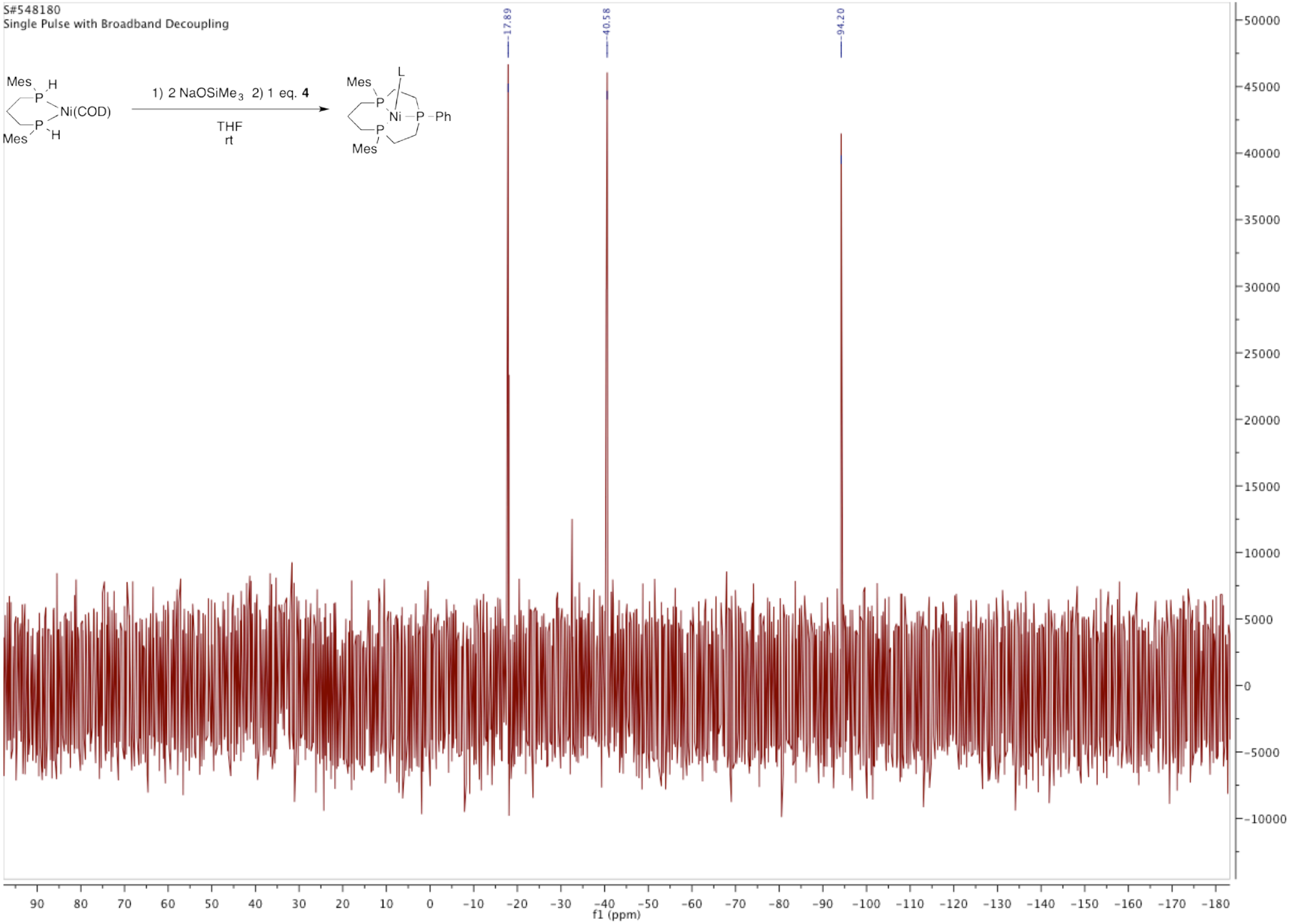

S#703506
Single Pulse Experiment
PH2
154.05
155.31
156.57
2800000
2600000
2400000
2200000
2000000
1800000
1600000
1400000
1200000
1000000
800000
600000
400000
200000
0
-200000
90 -95 -100 -105 -110 -115 -120 -125 -130 -135 -140 -145 -150 -155 -160 -165 -170 -175 -180 -185 -190 -195 -200 -205 -210
f1 (ppm)

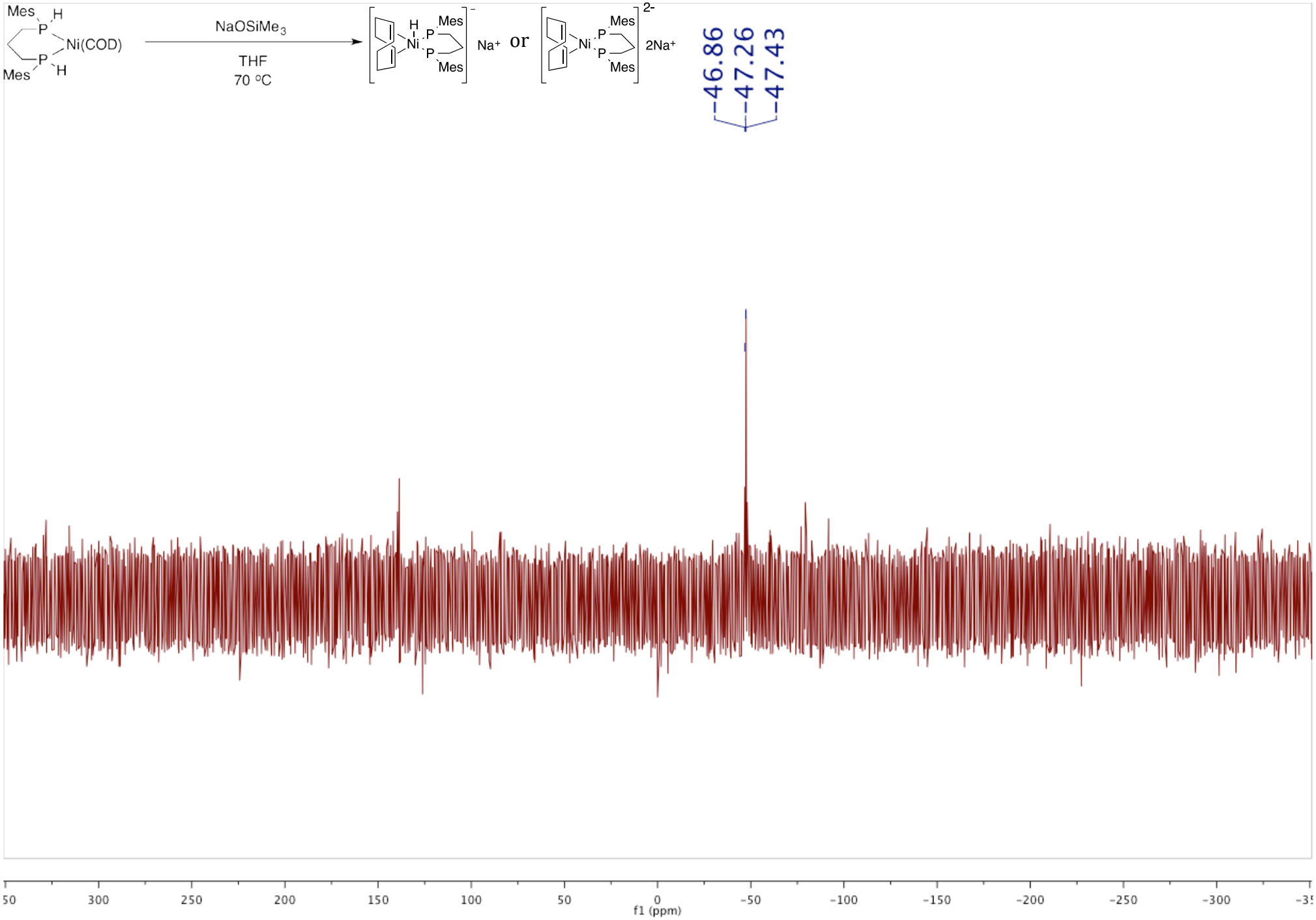

S#527110
Single Pulse with Broadband Decoupling
86.98
87.19
PH HP
Mes
Mes
6500000
6000000
5500000
5000000
4500000
4000000
3500000
3000000
2500000
2000000
1500000
1000000
500000
0
-500000
-1000000
-80
-81
-82
-83
-84
-85
-86
-87
-88
-89
-90
-91
-92
-93
-94
-95
-96
-97
-98
f1 (ppm)

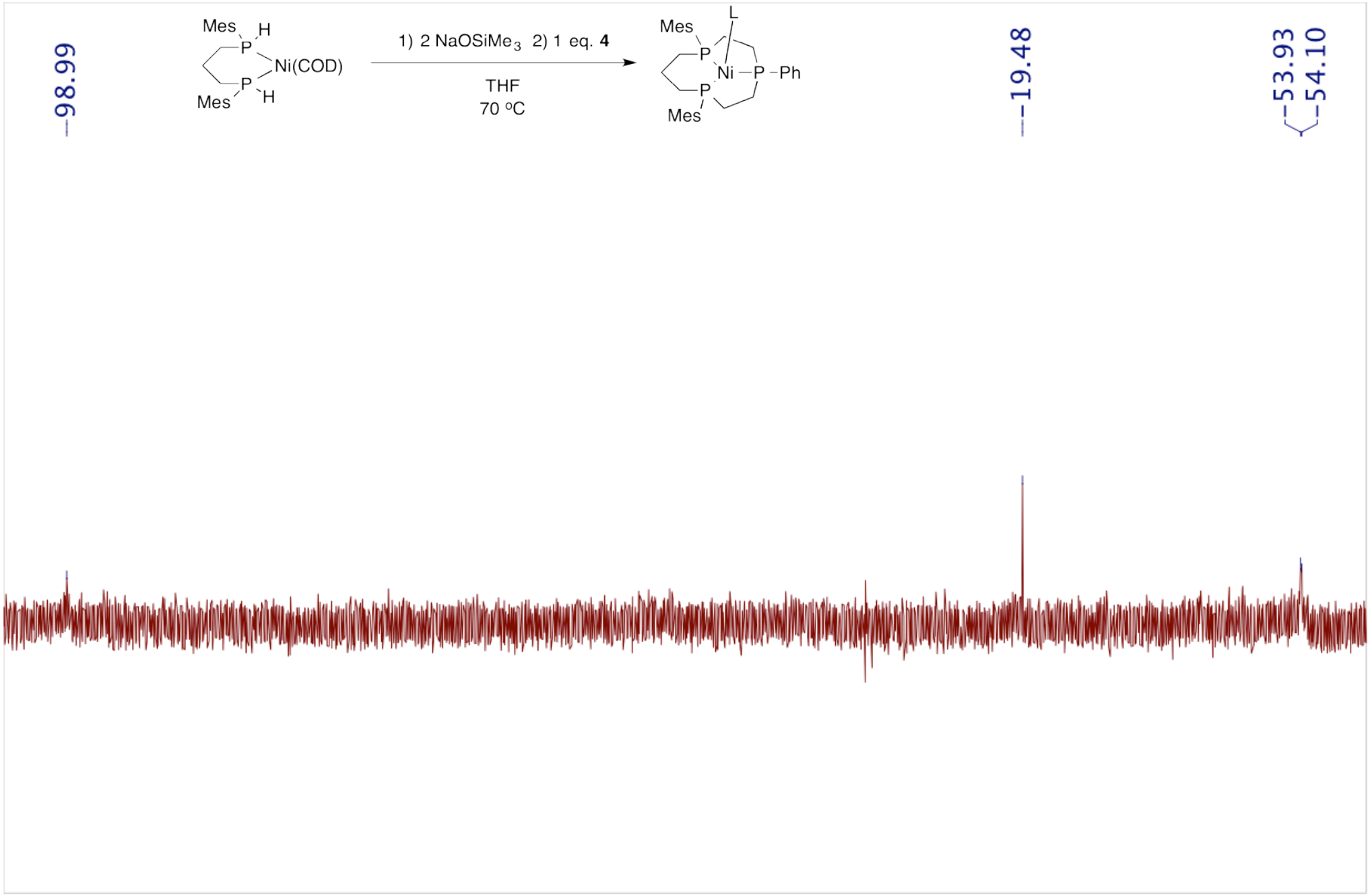

S#531248
Single Pulse Experiment
PH HP
Mes
Mes
86.30
86.33
86.53
86.56
87.62
87.66
87.84
87.87
650000
600000
550000
500000
450000
400000
350000
300000
250000
200000
150000
100000
50000
0
-50000
-83.5
-84.0
-84.5
-85.0
-85.5
-86.0
-86.5
-87.0
-87.5
-88.0
-88.5
-89.0
-89.5
-90.0
-90.5
-91.0
f1 (ppm)


S#555756
Single Pulse with Broadband Decoupling
20.64
25.44
Mes
H
P
Ni(COD)
P
Mes
H
1100000
1000000
900000
800000
700000
600000
500000
400000
300000
200000
100000
0
-100000
0
-5
-10
-15
-20
-25
-30
-35
-40
-45
-50
f1 (ppm)


S#780932
Single Pulse with Broadband Decoupling
Mes
H
P
Ni(COD)
P
Mes
H
+
P
Ph
THF
rt
Mes
H
P
Ni
P
P
Ph
Mes
H
21.39
26.20
32.05
37.90
38.26
39.85
40.08
44.20
44.56
f1 (ppm)


S#548180
Single Pulse with Broadband Decoupling
17.89
40.58
94.20
Mes
H
P
Ni(COD)
P
Mes
H
1) 2 NaOSiMe3 2) 1 eq. 4
THF
rt
L
Mes
P
Ni
P
Ph
P
Mes
50000
45000
40000
35000
30000
25000
20000
15000
10000
5000
0
-5000
-10000
90 80 70 60 50 40 30 20 10 0 -10 -20 -30 -40 -50 -60 -70 -80 -90 -100 -110 -120 -130 -140 -150 -160 -170 -180
f1 (ppm)


Mes
H
P
Ni(COD)
P
Mes
H
NaOSiMe3
THF
70 °C
H
Ni
P
Mes
P
Mes
Na+
or
Ni
P
Mes
P
Mes
2-
2Na+
-46.86
-47.26
-47.43
50
300
250
200
150
100
50
0
f1 (ppm)
-50
-100
-150
-200
-250
-300


-98.99
Mes
H
P
Ni(COD)
P
Mes
H
1) 2 NaOSiMe3 2) 1 eq. 4
THF
70 °C
L
Mes
P
Ni
P
Ph
P
Mes
-19.48
-53.93
-54.10
100
90
80
70
60
50
40
30
20
10
0
-10
-20
-30
-40
-50
-60
f1 (ppm)